journal

J. Am. Ceram. Soc., 76 [1] 3–28 (1993)

Corrosion of Silicon-Based Ceramics in Combustion Environments

Nathan S. Jacobson*

National Aeronautics and Space Administration, Lewis Research Center, Cleveland, Ohio 44135

Silicon-based ceramics and composites are prime candidates for heat engine and heat exchanger structural components. In such applications these materials are exposed to combustion gases and deposit-forming corrodents. In this paper combustion environments are defined for various applications. These environments lead to five main types of corrosive degradation: passive oxidation, deposit-induced corrosion, active oxidation, scale/substrate interactions, and scale volatility. Each of these is discussed in detail. The key issues in oxidation mechanisms of high-purity silicon carbide (SiC) and silicon nitride (Si_3N_4) in pure oxygen are discussed. The complicating factors due to the actual combustion environment and commercial materials are discussed. These discussions include secondary elements in the ceramics; additional oxidants, such as water and carbon dioxide (CO_2); combustion environment impurities; long-term oxidation effects; and thermal cycling. Active oxidation is expected in a limited number of combustion situations, and the active-to-passive transition is discussed. At high temperatures the limiting factors are scale melting, scale volatility, and scale/substrate interactions. Deposit-induced corrosion is discussed, primarily for sodium sulfate (Na_2SO_4), but also for vanadate and oxide-slag deposits as well. In applying ceramics in combustion environments it is essential to be aware of these corrosion routes and how they affect the performance of a component.

I. Introduction

MANY potential uses of silicon-based ceramics and composites involve exposure to combustion gases. These applications range from hot-section structural components of gas turbines and piston engines to heat exchanger tubes for industrial furnaces. Gas turbines are used in aircraft and electric power generation and have been tested for automobiles.[1] Potential ceramic components of these engines include combustor liners and, perhaps some day, turbine blades.[2,3] The location of these components in a gas turbine engine is shown in Fig. 1(a). In piston engines the potential ceramic components include valves and piston heads,[4] as shown in Fig. 1(b). The use of ceramic tubes as heat exchangers has been proposed for industrial furnaces, such as glass remelt furnaces, steel soaking pits, and aluminum reclamation furnaces.[5] An example is illustrated in Fig. 1(c). In addition, ceramics are under consideration for heat exchangers in coal-fired combustors.[6] A more developed application is the use of ceramic tubes for indirect heating, where hot combustion gases pass through the tube, heating a process on the outside.[7] The structural components of the hot sections are subject to a range of chemical attack processes, depending on the temperature, pressure, and chemical environment.

The focus of this paper is on the silicon-based ceramics silicon carbide (SiC) and silicon nitride (Si_3N_4). These materials are inherently unstable in air and form a thin layer of silicon dioxide (SiO_2) in an oxidizing environment. SiO_2 has the lowest permeability to oxygen of any of the common oxides and forms an effective reaction barrier.[8] Therefore, silicon-based ceramics have the potential of substantially better high-temperature oxidation behavior than metals. The protective oxide scales on silicon, SiC, and Si_3N_4 are shown schematically in Fig. 2. Note that Si_3N_4 forms a silicon oxynitride (Si_2N_2O) layer below the SiO_2 layer.[9] SiC may also form an oxycarbide layer, but there is only limited evidence for this.[10] The analogous protective layers on superalloys for high-temperature applications are alumina (Al_2O_3) and chromia (Cr_2O_3).[11] Extensive work has been done on the performance of Al_2O_3 and Cr_2O_3 scales in combustion environments. In general, our knowledge of the behavior of SiO_2 scales lags behind that of Al_2O_3 and Cr_2O_3.

The purpose of this paper is to review our current state of knowledge of the interaction of SiO_2 with combustion environments. Because the focus is on the interaction of SiO_2 with the environment, many of the conclusions apply to all SiO_2-protected materials. This includes composites of SiC and Si_3N_4, such as SiC-fiber-reinforced SiC matrices and SiC-fiber-reinforced Si_3N_4 matrices, and SiO_2-forming alloys, such as molybdenum disilicide ($MoSi_2$). In this paper the major chemical degradation routes are discussed. Particular emphasis is on the mechanisms of corrosion and the key questions involving them.

II. Environments

Combustion environments vary widely, depending on fuel, temperature, pressure, and oxidizer. Fuels are complex mixtures of hydrocarbons, and they are classified by boiling points. Lower-boiling-point fuels include automotive gasoline, and higher-boiling-point fuels include aviation fuel and fuel oils.[12]

S. M. Wiederhorn—contributing editor

Manuscript No. 195598. Received June 15, 1992; approved September 28, 1992.

*Member, American Ceramic Society.

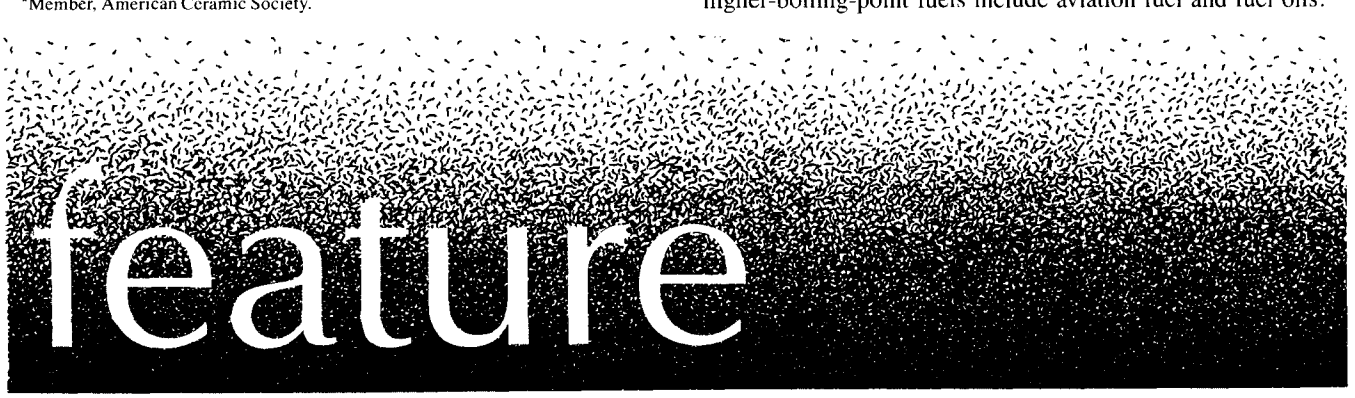

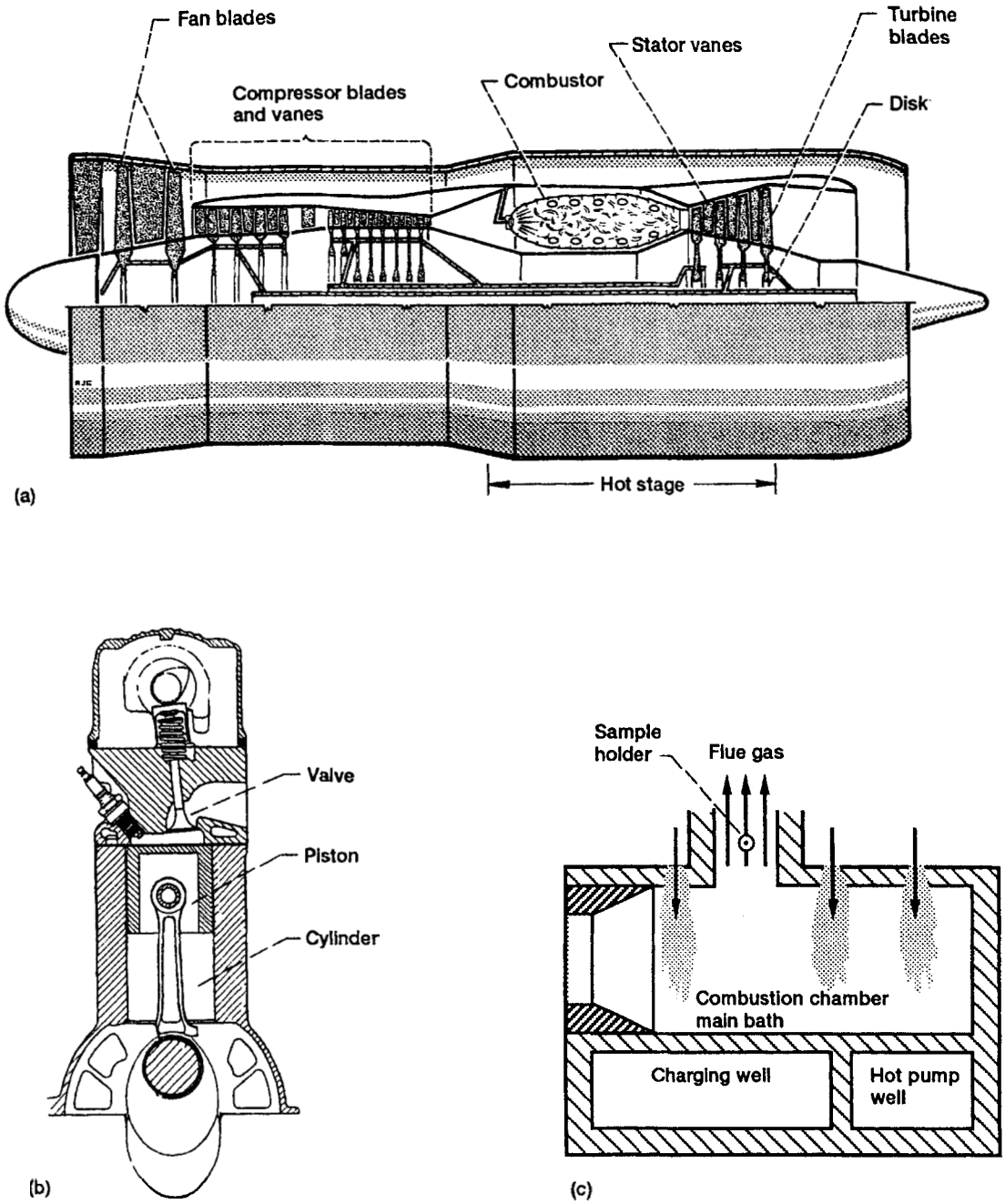

Fig. 1. Schematics of proposed applications for ceramics where ceramics will be subjected to combustion environments: (a) gas turbine engine, (b) piston engine, and (c) aluminum reclamation furnace (see Ref. 5).

Table I lists some common fuels and their approximate impurity contents.[13-16] Note that all fuels have some amount of sulfur, which may lead to corrosion. The last category of fuel oils contains more sodium, potassium, and vanadium than the other fuels. These lower-purity fuels are likely to be utilized more in the future as petroleum resources decrease. Impurities have a major influence on corrosion. Table I does not include coal-derived fuels, which generally have even higher impurity levels.

Combustion is the oxidation of these fuels to the stable products carbon dioxide (CO_2) and water (H_2O). Equilibrium combustion products can be calculated by mixing the fuel and the oxidant together in a free-energy-minimization computer code.[17] Figure 3(a) shows the equilibrium combustion products for a standard aviation fuel (Jet A—$CH_{1.9185}$) as a function of equivalence ratio. Equivalence ratio is defined as the fuel-to-air ratio at a particular point divided by the stoichiometric fuel-to-air ratio for complete combustion to CO_2 and H_2O. Thus, an equivalence ratio of 1 is stoichiometric, an equivalence ratio of less than 1 denotes a fuel-lean region, and an equivalence ratio greater than 1 denotes a fuel-rich region. Most gas turbines operate in the fuel-lean or stoichiometric regions. These regions contain large amounts of oxygen with the CO_2 and H_2O. Most corrosion studies have been performed in the fuel-lean region. However, some novel combustor designs may involve the fuel-rich region, which produces larger amounts of carbon monoxide (CO) and hydrogen gas (H_2). However, this region also contains the combustion products CO_2 and H_2O. Note that these are equilibrium calculations; if equilibrium is not attained, other species, such as elemental carbon, may form. The goal of a corrosion study is to understand the chemical reactions that occur between these combustion products and the proposed hot-gas-path structural materials.

Figure 3(b) shows the adiabatic flame temperature as a function of equivalence ratio. This temperature is calculated by using a free-energy-minimization computer code and setting

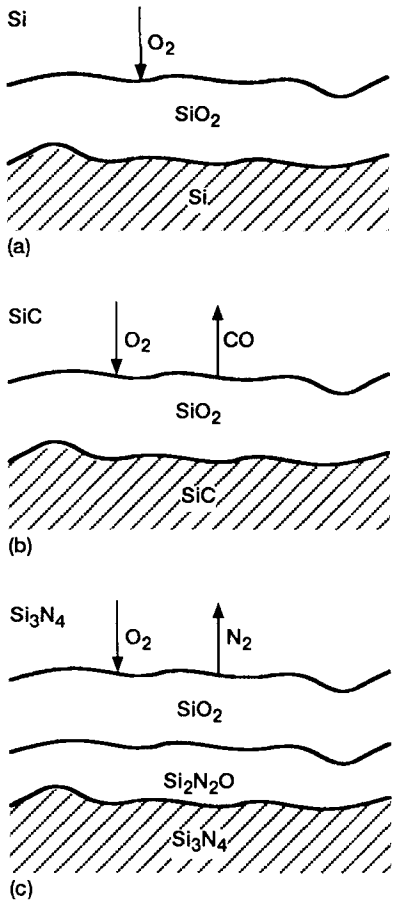

Fig. 2. Schematic of protective oxide scales: (a) on Si, (b) on SiC, and (c) on Si_3N_4.

the net heat loss equal to zero.[17] This is an idealized case that assumes no heat loss through the walls of the combustion chamber. It does give the maximum temperature of the flame, however. In general, the wall materials and the components downstream from the flame are at lower temperatures.

Corrosion occurs not only by gaseous combustion products, but also by deposits. Perhaps the most common deposit is sodium sulfate (Na_2SO_4), which forms when sodium reacts with sulfur fuel impurities.[18] The sodium may originate from a marine environment, from a salted roadway, or as a fuel impurity. Corrosion by Na_2SO_4 is termed "hot corrosion" and is discussed in detail herein. Other types of deposit-induced corrosion originate from vanadium fuel impurities and from oxide slags.

In some ways the piston chamber of an internal combustion engine is a more complex environment than the hot section of a gas turbine.[19] Pressures and temperatures vary through the stroke of the piston. Adiabatic flame temperatures and combustion gas product compositions can be calculated by the same free-energy-minimization program described previously with propane (C_3H_8) as a model fuel. The results of this calculation are similar to those for Jet A aviation fuel. Current automotive engines run slightly fuel rich to allow proper operation of pollution control devices.

In addition to heat engines, silicon-based ceramics are also prime candidates for heat exchanger tubes in industrial furnaces. The environment encountered by a heat exchanger varies widely. Again, one would expect large amounts of CO_2 and

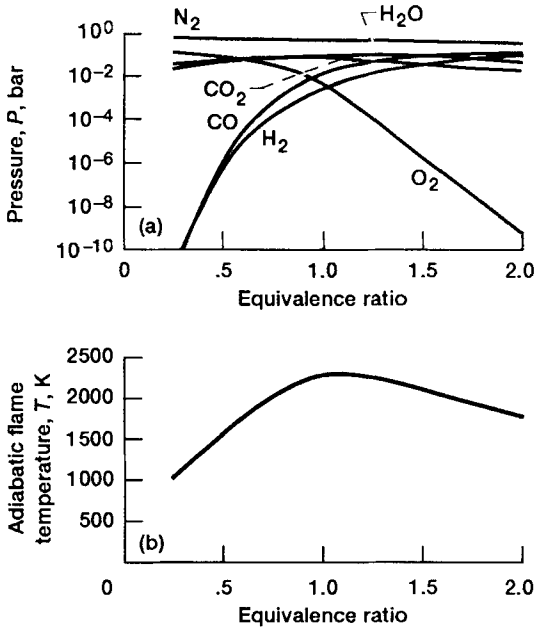

Fig. 3. Calculated gas composition and flame temperature as a function of equivalence ratio: (a) equilibrium gas composition and (b) adiabatic flame temperature.

H_2O, but now the impurities play a key role. An aluminum reclamation furnace and a glass remelt furnace may involve alkali-metal salts that can deposit on the heat exchanger.[5] In a coal-fired furnace the atmosphere may be more reducing.[6] In addition, a mixture of oxides may form a slag deposit, which can be quite corrosive, on the tubes.

Table II summarizes the composition of these combustion environments. This list is by no means exhaustive. As noted, specific applications generate specific corrodents. For example, combustion of municipal wastes may generate hydrogen chloride (HCl).[20] In summary, combustion environments are complex, involving not only the combustion products CO_2 and H_2O, but a variety of other gases and possible deposits as well.

Temperatures and pressures are again quite dependent on the particular system. The ranges are listed in Table II. An important issue to consider is thermal cycling. Some applications, such as a utility turbine or industrial furnace, involve essentially isothermal exposures for long periods. Other applications, such as an aircraft gas turbine, involve thermal cycling.

III. Types of Corrosive Attack and Experimental Techniques

Figure 4 shows the major types of corrosive attack as a function of pressure and reciprocal temperature. The major types of corrosive degradation are passive oxidation, deposit-induced corrosion, active oxidation, oxide/substrate interactions, and scale vaporization. The temperature boundaries between these types are only approximate and are dependent on the specific system. Furthermore, rarely is one mechanism operative. In practice, several mechanisms operate simultaneously.

Laboratory studies of corrosive degradation fall into two main categories: burner rig studies and laboratory furnace studies. Burners more accurately model the actual combustion situation. Figure 5 shows a typical high-velocity burner rig.

Table I. Properties of Some Common Hydrocarbon Fuels

Fuel	Boiling range (K)*	H:C molar ratio†	S content (wt%)‡	Na + K content (ppm)§	V content (ppm)¶
Unleaded automotive gasoline	300–375	2.02	0.15	3.6	<0.003
Jet A (commercial aviation fuel)	450–560	1.92	0.05	~10	0.06
Fuel oils	450–615	1.61	0.1–1.0	10–20	<300

*Reference 12. †Reference 13. ‡References 14 and 15. §Reference 15. ¶References 15 and 16.

Table II. Summary of Combustion Environments

Application	Temperature (K)	Pressure (bar)†	Gas atmosphere	Potential deposit
Heat engines				
Gas turbine	1173–1673	1–50	Fuel lean: N_2, O_2, CO_2, H_2O; fuel rich: N_2, CO_2, H_2O, CO, H_2	Na_2SO_4, $Na_2V_xO_y$
Piston	1273–1873‡	1–10	N_2, CO_2, H_2O, O_2	
Heat exchanger	1273–1873	~1	Oxidizing	Alkali halides, Na_2SO_4, transition-metal oxides
Coal combustion	1473–1673	1–10	Reducing	Acidic or basic coal slags

†1 bar = 10^5 Pa. ‡Cycling.

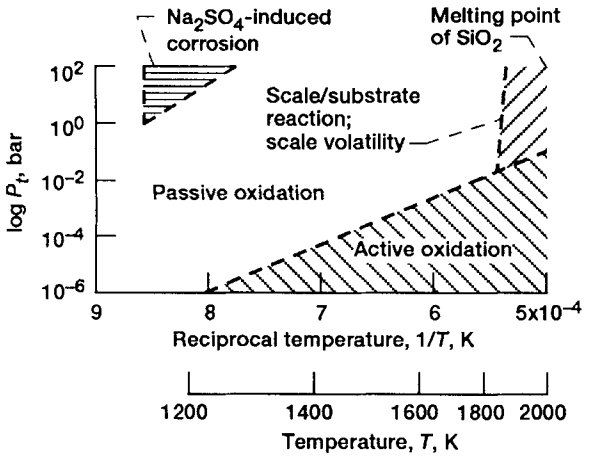

Fig. 4. Major types of corrosive attack and degradation as an approximate function of reciprocal temperature ($P_{total} = P_{oxidant}$).

However, burner rig tests are expensive, and it is difficult to precisely control all the operating parameters. Laboratory furnace tests offer much more accurate control of system parameters. Gas composition, pressure, and temperature can be accurately controlled. The extent of corrosion can be monitored by following the weight gain with a microbalance or by measuring scale thickness with various optical techniques. Figure 6 shows a standard laboratory microbalance apparatus for isothermal oxidation studies. Standard electron–optical techniques have been useful for characterizing corroded specimens. In general, burner rig tests are helpful for an overall assessment of behavior in the actual environment. Laboratory furnace tests complement burner rig tests by permitting isolation of individual effects so that they can be understood on a fundamental basis.

IV. Isothermal Oxidation

(1) General Considerations and Pure Silicon Oxidation

A large amount of research has been performed on the isothermal, passive oxidation of silicon-based ceramics. This research is complex because of the various secondary effects, such as other oxidants and impurities in the ceramics and the environment. These effects are noted in Fig. 7. Fundamental studies are at the center of the circle—pure materials and pure oxygen environments. Eliminating the complicating factors allows detailed studies of the basic oxidation mechanism. Actual combustion environments are more complex, involving the various factors on the outer circle in Fig. 7.

The focus of this section is on fundamental studies of SiC and Si_3N_4 oxidation. These studies provide an atomistic understanding of the mechanism of SiO_2 scale growth. These include determining the slow reaction step (or steps) and understanding the diffusion mechanism. Despite the large number of papers in this area, many questions remain unanswered. This paper is not intended to be an exhaustive review but rather a discussion of some of the key issues involved.

SiO_2 has some unique properties that influence its performance as a protective oxide. In most oxidation experiments, SiO_2 forms as an amorphous film and then crystallizes to either cristobalite or tridymite. This is significant because these phases have very different physical and chemical properties.[21] It is generally accepted that the mobile species is oxygen, not silicon. For this reason the chemical reaction occurs at the SiO_2/Si or SiO_2/ceramic interface.[22,23] Transport through SiO_2 can occur by diffusion of molecular oxygen as interstitials or by network exchange of ionic oxygen.[24,25] The latter is referred to as either "network exchange diffusion" or "ionic diffusion" in this paper. Molecular oxygen diffusion coefficients are measured by examining permeation through a SiO_2 membrane;[26] network exchange diffusion coefficients are measured by an isotope exchange technique.[27–29] Table III lists both types of diffusion coefficients. The molecular oxygen diffusion coefficient is roughly 10^6 times greater than the ionic oxygen diffusion coefficient. There have been attempts to correlate these two types of diffusion coefficients;[24] however, Cawley[30] has reported the difficulties with such a correlation due to network/interstitial exchange and mobile network ions. These issues and the disparity of the diffusion coefficient measurements (Table III) indicate there are still some unresolved issues in these fundamental transport quantities.

Before discussing the oxidation of SiC and Si_3N_4, it is appropriate to discuss the oxidation of pure silicon. Because this process is critically important to the semiconductor industry, it has been extensively studied. The classic paper in this area is by Deal and Grove.[31] They view oxidation as consisting of three distinct steps, as shown in Fig. 8. The three steps are transfer of the gaseous oxidant to the outer surface of the oxide film, diffusion through the oxide film, and reaction at the oxide/silicon interface. From these steps they derive the following linear–parabolic equation:

$$x^2 + Ax = B(t + \tau) \tag{1}$$

where x is the scale thickness, B the parabolic rate constant, t the time, and τ the time shift corresponding to the presence of an initial oxide layer. The quantity B/A is the linear rate constant. The parabolic rate constant is given by

$$B = 2D_{eff}C^*(O_2)/N_O \tag{2}$$

where D_{eff} is the diffusion coefficient through the film, $C^*(O_2)$ is the equilibrium concentration of oxidant in the scale, N_O the number of oxygen molecules incorporated into the SiO_2 scale per unit volume. Note that N_O must be modified for SiC oxidation due to the formation of CO. For short oxidation times, oxidation follows a linear rate law. The physical interpretation of this linear region is still controversial; it has been attributed to interface control[31] or to diffusion control which is nonparabolic due to strain effects in the oxide.[32] For longer times, oxidation follows a parabolic law, and diffusion through the thicker oxide is rate controlling. An activation energy can be determined from a plot of ln B vs $1/T$. The magnitude of the activation energy can reveal useful information about the diffusion process. Deal and Grove[31] report that care must be taken to interpret the oxidation process at the appropriate times (i.e., parabolic behavior cannot be assumed when the process is still in the linear region). They have shown that Eq. (1) describes a

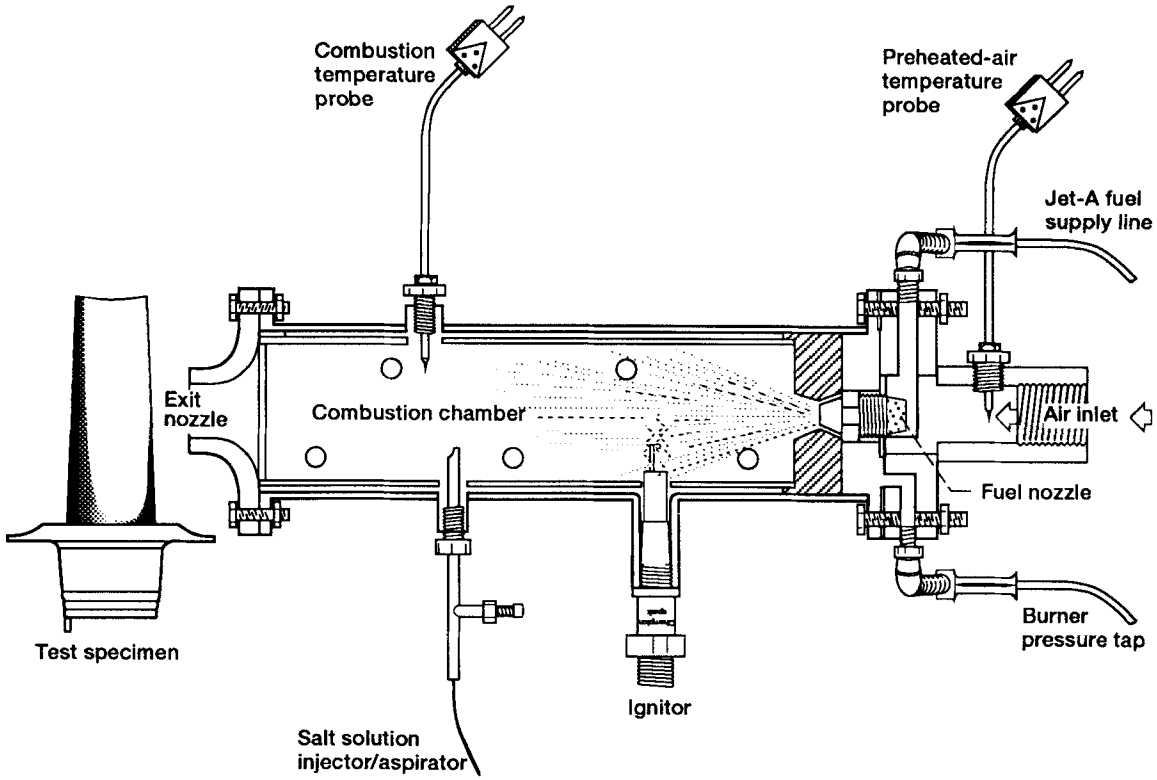

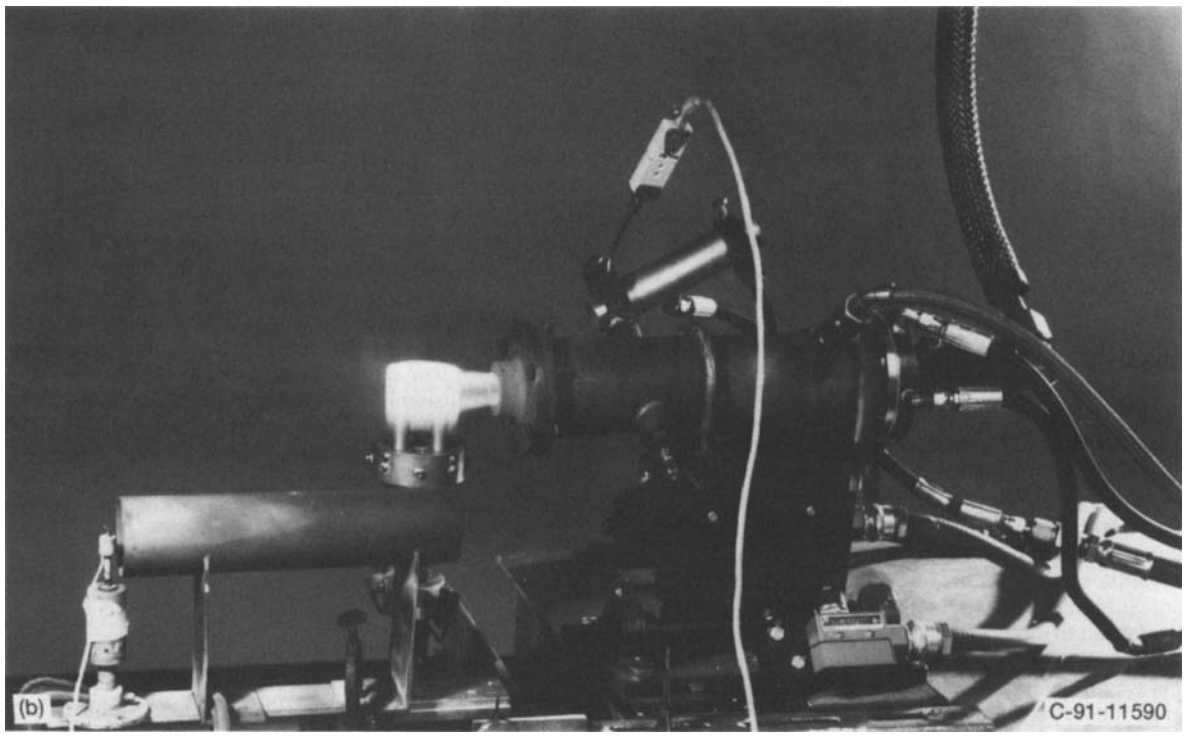

Fig. 5. Mach 0.3 burner rig. (Courtesy of M. Cuy, NASA Lewis.)

wide range of oxidation data. Calculations of the parabolic rate constant that are based on the molecular oxygen diffusion coefficient of Norton[26] show good agreement with the measured values, and the activation energy for parabolic oxidation is close to that for molecular oxygen diffusion through SiO_2. Thus, it is generally accepted that molecular oxygen diffusion through the SiO_2 layer is rate controlling.[33,34]

The oxidation of SiC and Si_3N_4 is more complex. Figure 2 illustrates some of the processes involved. In both ceramics there is a countercurrent of gas. The following reactions are generally accepted:

$$SiC(s) + 1.5O_2(g) = SiO_2(s) + CO(g) \quad (3)$$

$$Si_3N_4(s) + 0.75O_2(g) = 1.5Si_2N_2O(s) + 0.5N_2(g) \quad (4a)$$

$$Si_2N_2O(s) + 1.5O_2(g) = 2SiO_2(s) + N_2(g) \quad (4b)$$

However, the actual processes may involve other reactions. The production of CO in the oxidation of SiC has been observed

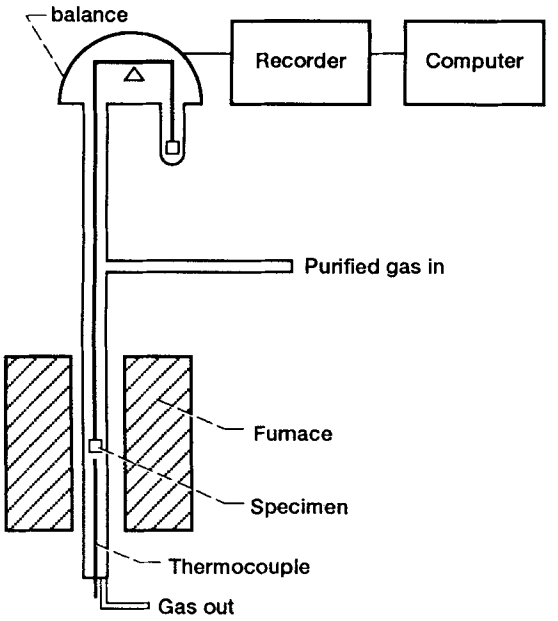

Fig. 6. Schematic of oxidation balance apparatus.

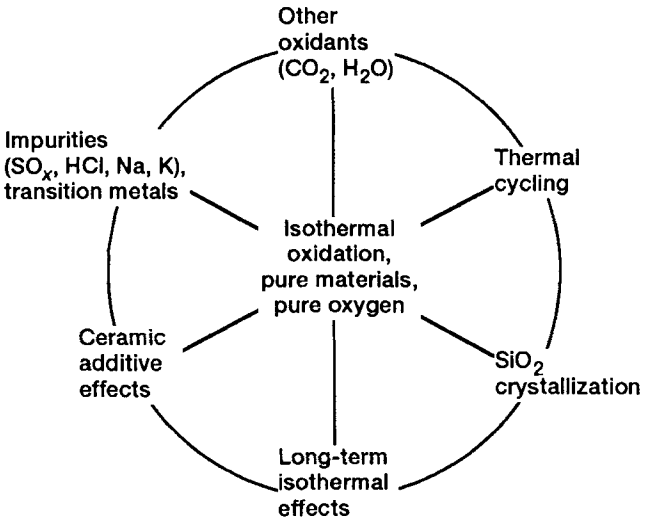

Fig. 7. Complications to isothermal oxidation due to additive-containing ceramics and combustion environments.

with the gas chromatograph,[35] although the possibility of further oxidation to CO_2 must be considered. There has been no clear observation of the production of elemental carbon. The oxidation of Si_3N_4 may lead to the production of nitrous oxide (NO(*g*)) in addition to molecular nitrogen gas, as observed with a mass spectrometer.[36,37] Note that, even though the reactions lead to a net weight gain, there is also some weight loss due to gas evolution. These reactions may be monitored by following net weight gain, scale thickness as a function of time, or even gas evolution. The following factors allow conversion of parabolic rate constants from scale thickness to net weight gain:[38]

$$1\ (m^2/s) = 1.67 \times 10^{-6}\ (kg^2/(m^4 \cdot s)) \quad \text{for SiC} \quad (5)$$

$$1\ (m^2/s) = 3.77 \times 10^{-6}\ (kg^2/(m^4 \cdot s)) \quad \text{for } Si_3N_4 \quad (6)$$

Note that Eq. (5) is based on Eq. (3) and that Eq. (6) is based on a combination of Eqs. (4*a*) and (4*b*), i.e., the oxidation of Si_3N_4 to SiO_2. This is appropriate since SiO_2 is formed in much larger amounts than Si_2N_2O.[9]

The oxidation process for SiC and Si_3N_4 involves five steps: (1) transport of molecular oxygen gas to the oxide surface, (2) diffusion of oxygen through the oxide film, (3) reaction at the oxide/ceramic interface, (4) transport of product gases (e.g., CO and nitrogen) through the oxide film, and (5) transport of product gases away from the surface. This process is even more complex in the Si_3N_4 case because of the duplex film formation. Many questions remain about these steps. The key question concerns the rate-controlling, or slowest, step. This has been an area of controversy for both SiC and Si_3N_4 and is discussed in further detail herein. Another question deals with the transport mechanism through the SiO_2 scale. Is it permeation through the network by oxygen molecules or a network exchange mechanism of O^{2-}? Even less is known about the transport mechanism of product gases (CO and nitrogen) outward through the SiO_2 scale. As noted, SiO_2 undergoes a number of phase changes. This section deals primarily with amorphous scales. Crystallization, which complicates the oxidation process, is discussed separately.

(2) Silicon Carbide

First consider the oxidation of SiC. The key observations have been summarized by several investigators.[38–40] Generally, only one scale forms, although there is limited evidence that an oxycarbide may form between the oxide and the SiC.[10] Figure 9 shows a representative kinetic curve. Many investigators have observed a brief ($<<1$ h) linear region followed by a parabolic region.[41–45] The focus of most investigations has been on the parabolic region, as shown in Fig. 9. Figure 10 shows the parabolic rate constants for a number of SiC materials. Only the higher-purity materials (i.e., chemically-vapor-deposited (CVD) SiC and single-crystal SiC) are discussed in this section.

The key question concerns the rate-controlling step. There are three possibilities: (1) oxygen diffusion inward, (2) CO diffusion outward, and/or (3) an interfacial reaction. Recently, Luthra[38] systematically examined these possibilities based on available experimental data. His general approach is taken here. Table IV summarizes some of the experimental observations and their implications.

(A) Oxygen Diffusion Inward: In general, most of the data imply oxygen diffusion inward as rate limiting. Rates are parabolic and dependent on the partial pressure of oxygen (P_{O_2}). Motzfeld[46] has reviewed the literature to about 1963 and carefully compared the rate constants for silicon and SiC. After correcting for the stoichiometry difference (i.e., the additional oxygen necessary to oxidize carbon), he finds that silicon and SiC have essentially the same rates and the same activation energies. Therefore, he concludes that the same process that controls silicon oxidation also controls SiC oxidation (i.e., oxygen diffusion inward). Much of the data he uses are for SiC powder. The difficulty in a precise determination of the surface area and possible impurities suggests that high-purity coupons may give more precise data for SiC. Recent measurements on single-crystal SiC[47] give rates somewhat slower than those for silicon, as shown in Fig. 10.

Table V summarizes the activation energies for oxidation of high-purity SiC. Note that there is generally a low-temperature ($T < 1623$ K) and a high-temperature ($T > 1623$ K) regime. Consider the low-temperature regime. Here the activation energy is low, about 120 to 140 kJ/mol, and is similar to that for oxidation of pure silicon and molecular oxygen diffusion through amorphous SiO_2. This supports molecular oxygen diffusion inward as a rate-controlling step for SiC oxidation below 1623 K.

Consider further the type of transport through the growing SiO_2 layer. As mentioned, the activation energy for oxidation becomes much greater after 1623 to 1673 K for controlled-nucleation thermally deposited (CNTD) SiC and the carbon face of single-crystal SiC. Zheng *et al.*[47,48] have explained this phenomenon as a change in the oxygen transport mechanism. Below about 1623 K, the activation energy for the parabolic rate constant is close to that for silicon oxidation, and diffusion of molecular oxygen through the scale is rate controlling. They show this by forming a scale in ^{16}O and then reoxidizing in ^{18}O.

Table III. Diffusion Coefficients for Oxygen in Amorphous SiO_2

Investigator	Technique	Type of diffusion coefficient, temperature range (K)	Diffusion coefficient value (m^2/s)
Norton[26]	Permeation	Molecular O_2, 973–1373	$2.9 \times 10^{-8} \exp(-112900/RT)$
Williams[28]	Isotope exchange	Network exchange, 1123–1523	$2.0 \times 10^{-13} \exp(-121336/RT)$
Sucov[27]	Isotope exchange	Network exchange, 1198–1498	$1.5 \times 10^{-6} \exp(-297901/RT)$
Muehlenbachs and Schaeffer[29]	Isotope exchange	Network exchange, 1423–1703	$4.4 \times 10^{-15} \exp(-82425/RT)$

[a] E^* in J/mol.

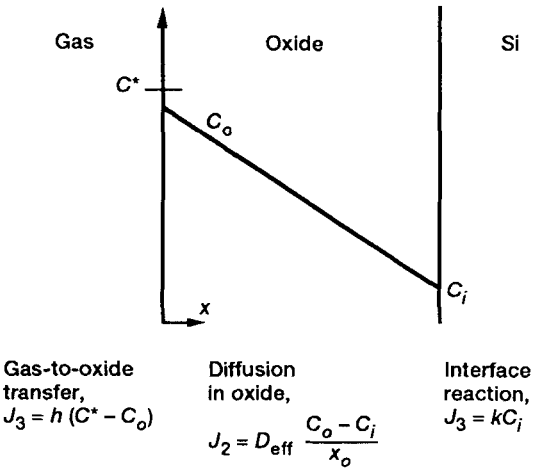

Fig. 8. Processes involved in silicon oxidation. (After Deal and Grove.[31])

An accumulation of ^{18}O at the SiO_2/SiC and SiO_2/gas interface, as determined by secondary ion mass spectrometry (SIMS), supports this. Above 1673 K the activation energy becomes higher, and this is attributed to a mixture of network exchange diffusion and molecular oxygen diffusion. Zheng *et al.*[47,48] have observed a constant distribution of ^{18}O through the scale in their reoxidation experiment. They attribute this to the exchange process. However, Cawley and Boyce[49] have reported that, without some type of concentration gradient, it is difficult to draw conclusions about the diffusion mechanism.

A transition from molecular oxygen to network oxygen diffusion should be reflected in the dependence of the parabolic rate constant k_p on P_{O_2}. For molecular oxygen diffusion, the rate constant should be proportional to P_{O_2}, assuming that the solubility of oxygen in SiO_2 obeys Henry's law. For network exchange diffusion, one expects k_p to show a weak dependence on P_{O_2}.[48,50] Zheng *et al.*[48] have found k_p to be dependent on $(P_{O_2})^n$, where n varies from 0.6 at 1473 K to 0.3 at 1773 K. This variation is generally consistent with the proposed transition between the two types of diffusion. At lower temperatures one might expect a value of n closer to 1 for molecular oxygen diffusion. Zheng *et al.* attribute the difference to deviations from Henry's law for the solubility of oxygen in SiO_2. Narushima *et al.*[51] have found k_p to be proportional to $(P_{O_2})^{1/2}$ at 1823 to 1948 K. From the high activation energy, Narushima *et al.* conclude that network exchange diffusion of oxygen inward is rate controlling.

In the case of network exchange diffusion, the expected P_{O_2} dependence is important to explore further. Using standard Kröger–Vink notation and assuming that oxygen vacancies are the primary defect,

$$O_O = V_O^{\cdot\cdot} + 2e' + 0.5O_2 \tag{7a}$$

$$[V_O^{\cdot\cdot}] = K' P_{O_2}^{-1/6} \tag{7b}$$

$$D_O = D_O^O P_{O_2}^{-1/6} \tag{8}$$

According to the Wagner oxidation theory[50] for ionic diffusion,

$$k_p = \frac{K''}{2} \int_{P_{i,O_2}}^{P_{g,O_2}} D_O \, d \ln P_{O_2} = 3K'' D_O^O (P_{i,O_2}^{-1/6} - P_{g,O_2}^{-1/6}) \tag{9}$$

$$\approx 3K'' D_O^O P_{i,O_2}^{-1/6}$$

where the subscripts i and g refer to the SiC/SiO_2 interface and SiO_2/gas interface, respectively; D_O is the diffusivity of oxygen; and the K' and K'' are constants. Equation (9) simplifies since $P_{g,O_2} >> P_{i,O_2}$ and there is a negative vacancy gradient as described by Eq. (7*b*). Thus, k_p shows very little dependence on external P_{O_2}. This is in accordance with the oxidation literature for scale growth on materials with this type of oxide defect structure.[50] The change in P_{O_2} dependence of k_p with temperature[48] is consistent with a transition from molecular diffusion to a larger contribution of ionic diffusion. Note also that, with a defect structure different from that in Eq. (7*a*), the P_{O_2} dependence of k_p changes.

(B) CO Diffusion Outward: Some investigators have attributed the higher activation energies at higher temperatures to a transition to CO-diffusion-outward rate control.[35,52] Two factors tend to discount this. Zheng *et al.*[47] have oxidized $Si^{13}C$ and examined the resultant scale by using SIMS. They found no carbon gradient, as one would expect if CO diffuses outward slowly. Thermodynamic arguments also support the rapid transport of CO outward. Suppose the reverse is true and CO diffuses outward slowly. Then P_{O_2} at the SiC/SiO_2 interface must be close to 1, and, as required by diffusion control, Eq. (3) equilibrium is maintained; the P_{CO} has a value of about 10^{27} bar (1 bar = 10^5 Pa) at 1600 K. Extremely high pressure would be expected to blow the scale off, but this is not observed. Some type of "CO pressure gauge" is needed at the SiC/SiO_2 interface. The formation of bubbles in the scale may provide some indication of pressure buildup.[38] However, there are two difficulties with this. First, the precise pressure to form a bubble is not clear—it depends on local surface tension and a variety of other factors. Second, the source of bubbles at high temperatures may also be the SiC + SiO_2 reaction,[41] as discussed later in this paper.

(C) Interfacial Reaction: The other possibility for rate control is interfacial reaction. Some investigators have reported linear reaction rates for the silicon face of single-crystal SiC, which is attributed to interfacial reaction control.[53] However, most of the data for pure SiC indicate parabolic kinetics for the majority of the reaction period. Table IV summarizes the experimental observations and the rate-controlling step supported. Most of the evidence implies oxygen diffusion inward as being rate controlling.

However, the situation is not so clear. The most recent data indicate that single-crystal SiC has rates slower than that of pure silicon, even with the stoichiometry correction. The (0001) silicon face of single-crystal SiC shows rates slower than that of the $(000\bar{1})$ carbon face.[47] There is no explanation for this. Furthermore, the assumption of oxygen diffusion inward and CO diffusion outward assumes that one is fast and the other is slow. Although CO is polar and molecular oxygen is not, it is difficult to imagine that they would have dramatically different permeation properties. These three facts make it difficult to accept oxygen diffusion inward as completely rate controlling. Physical phenomena do not always fall into distinct categories. As Luthra[38] reports, it may be that a mixed control mechanism is operative and both diffusion and the interface

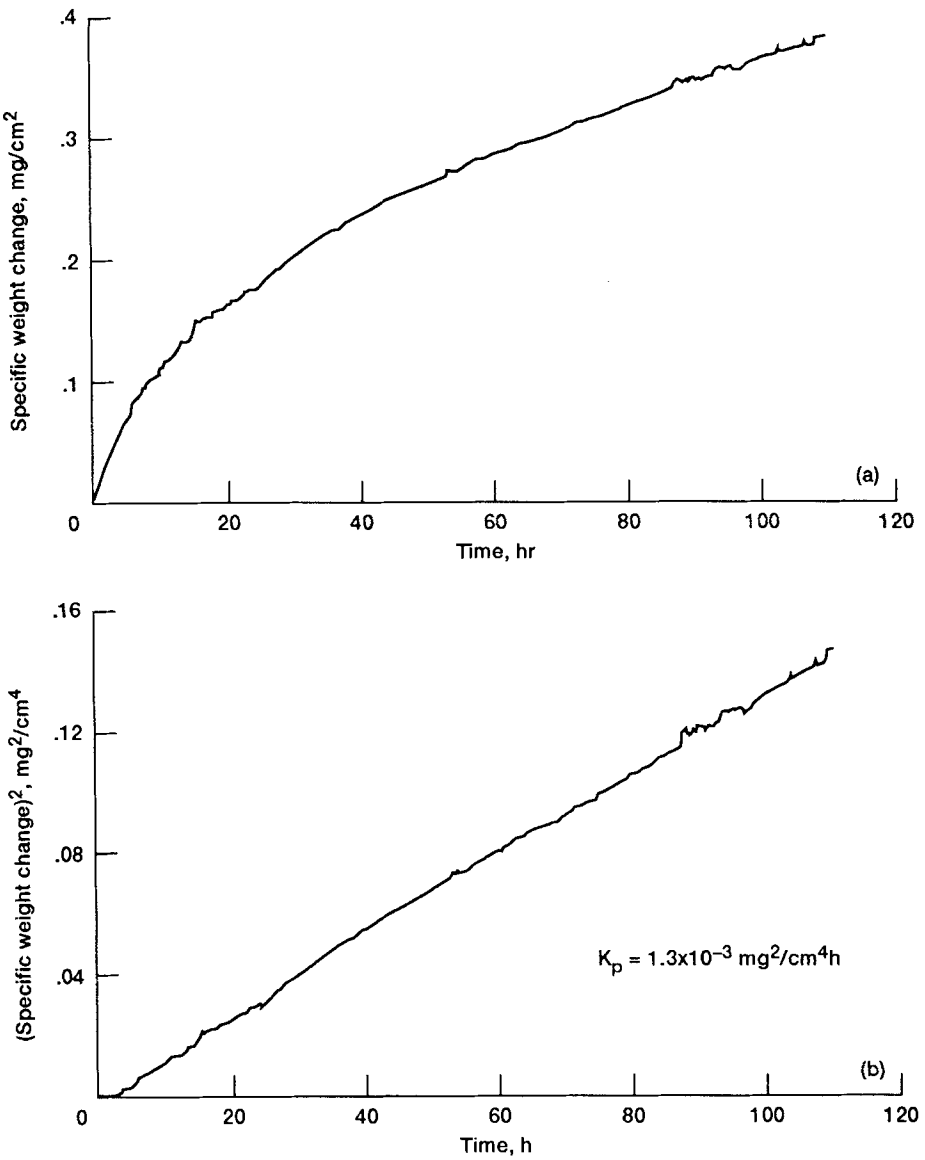

Fig. 9. Sample oxidation curves for CVD SiC in dry oxygen (T = 1673 K):[45] (a) weight gain versus time (1 mg/cm^2 = 10^2 kg/m^2) and (b) (weight gain)^2 versus time (1 mg^2/(cm^4·h) = 3.6×10^7 kg^2/(m^4·s)).

reaction are rate controlling. Because of the different rates of single-crystal SiC and silicon, Luthra advocates mixed interface and CO diffusion outward control. However, the limited evidence for high CO pressures at the SiO_2/SiC interface and lack of a carbon gradient tend to oppose CO diffusion outward. More work is necessary to determine the rate-controlling step (or steps).

(3) Silicon Nitride

Next consider Si_3N_4 oxidation. This is more complex because of the duplex layer formation. Figure 11 shows the parabolic rate constants for a range of Si_3N_4 materials. As in the SiC case, the focus in this section is on the high-purity materials (i.e., CVD Si_3N_4). Perhaps the most obvious thing about the CVD Si_3N_4 material is the steeper slope—the activation energy is substantially more than that for pure silicon. Table VI lists some activation energies for CVD Si_3N_4. In addition, the rates are slower than those for pure silicon and pure SiC for short oxidation times (~5 h) below about 1700 K; above 1700 K the rates are similar. These facts suggest that the oxidation mechanism for Si_3N_4 is different from that for SiC.

Luthra[38] has also systematically investigated the possible rate-controlling steps for Si_3N_4. Most investigators have observed parabolic kinetics, suggesting that either oxygen diffusion inward is rate limiting or nitrogen diffusion outward is rate limiting.[9,41,54-55] The parabolic rate constant varies linearly with oxygen pressure[9] at 1523 to 1673 K, and this variation suggests a molecular oxygen diffusion mechanism. Du *et al.*[56] have performed double oxidation experiments with $^{18}O_2$ and $^{16}O_2$ and suggest that permeation by molecular oxygen is the primary diffusion mechanism and that considerable exchange with the network occurs at higher temperatures. The higher activation energies for Si_3N_4 as compared with silicon (Table VI) have been attributed to oxygen transport through Si_2N_2O.[57] As in the SiC case, rate control by diffusion of a gaseous product outward is unlikely because this would create a very large nitrogen pressure at the oxide/nitride interface. Oxidation studies at very high temperatures show only limited bubbling.[41] An interfacial reaction-rate-limiting step is not likely because linear rates have not been clearly observed. Table VII summarizes the experimental observations and the rate-controlling steps. Again, most of the data support oxygen diffusion inward as a rate-controlling step, but there are some inconsistencies, as are shown below.

The difficulty with oxygen diffusion inward as a rate-controlling step arises from the substantially slower rates of Si_3N_4 as

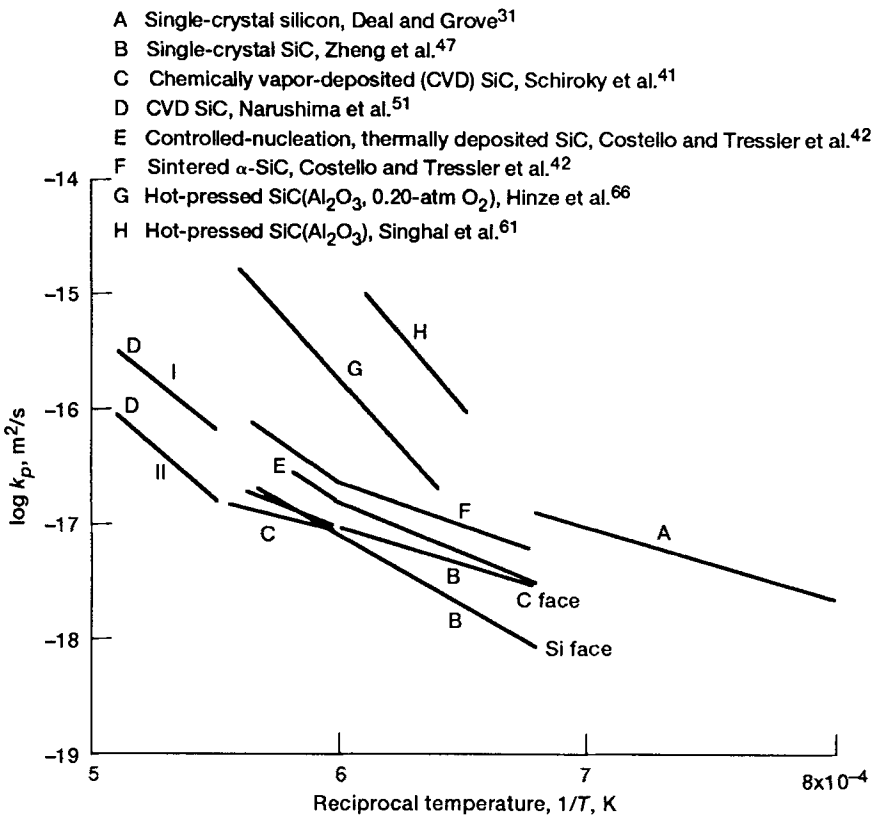

Fig. 10. Parabolic rate constants for a variety of SiC materials.

Table IV. Rate-Controlling Steps for SiC Oxidation

Observation	Observations support: Oxygen diffusion inward	Interfacial reaction	CO diffusion outward	Reference(s)
Parabolic kinetics	✓		✓	41, 42, 46, 47, 51
$k_p \propto p_{O_2}^n$ $(0.3 < n < 0.5)$	✓	✓		47
Double oxidation				
^{18}O at SiC/SiO_2 (low T)†	✓			47
Even distribution of ^{18}O (high T)‡				47
Oxidation of $Si^{13}C$; no accumulation of ^{13}C at SiC/SiO_2	✓			47
No clear indication of large P_{CO} at SiC/SiO_2	✓			51
Activation energy $E^*(SiC) \approx E^*(Si)$ (low T)†	✓			42,47
Rate constants				
$k_p(Si) > k_p(C\ face - SiC)$		✓	✓	47
$k_p(C\ face) > k_p(Si\ face)$	✓	✓	✓	42, 44, 47

†Permeation of O_2. ‡Network exchange of O^{2-}?.

Table V. Activation Energies for SiC Oxidation

Investigators	Temperature range (K)	Activation energy, E^* (kJ/mol)
Deal and Grove[31] (Si)	1073–1473	119.3
Costello and Tressler[42] (CNTD SiC)	1473–1673	142
Zheng *et al.*[47] (single-crystal SiC)	1673–1773	293
C face	1473–1623	120
C face	1623–1773	260
Si face	1473–1773	223–298
Schiroky *et al.*[41]	1640–1820	125.5
Narushima *et al.*[51]	1823–1948	345

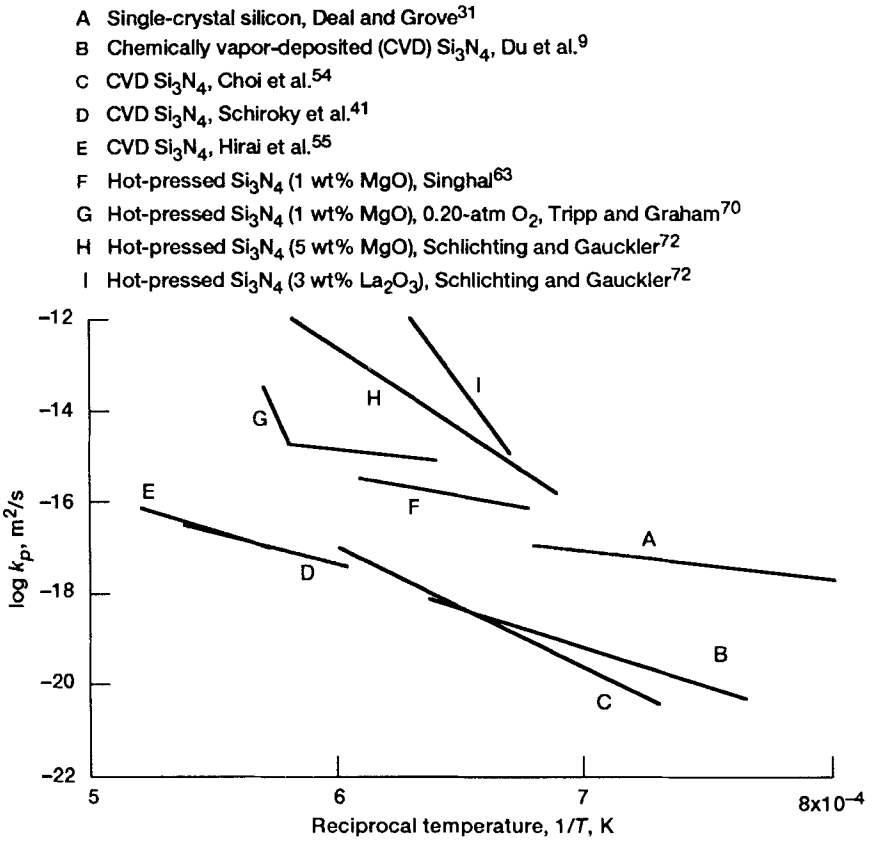

Fig. 11. Parabolic rate constants for a variety of Si_3N_4 materials.

Table VI. Activation Energies for Si_3N_4 Oxidation

Investigators	Temperature range (K)	Activation energy, E^* (kJ/mol)
Deal and Grove[31] (Si)	1073–1473	119.3
Du *et al.*[9]	1373–1673	464
Choi *et al.*[54]	1273–1573	330
Hirai *et al.*[55]	1823–1923	420
Schiroky *et al.*[41]	1673–1873	276

Table VII. Rate-Controlling Steps for Si_3N_4 Oxidation

Observation	Observations support: Oxygen diffusion inward	Interfacial reaction	Nitrogen diffusion outward	Reference(s)
Parabolic kinetics*	✓		✓	9, 54, 55
Activation energy				
$E^* > E^*$ (Si, SiC)	?		?	9, 54
$k_p \propto P_{O_2}$	✓			9
k_p not $f(P_{N_2})$	✓			9
No indication of large P_{N_2} at SiO_2/Si_3N_4	✓			41

*Some deviations from parabolic kinetics–some influence of interface (?).

compared with silicon. This fact leads to unreasonably high pressures at the SiO_2/Si_2N_2O interface. This has been discussed by both Du *et al.*[57] and Luthra[38] and the argument follows. The oxygen pressure dependence and double oxidation experiments suggest that, at low temperatures, molecular oxygen diffusion occurs for silicon and Si_3N_4. Because the Si_2N_2O layer is only about one-tenth of the SiO_2 layer, consider the parabolic growth rate of the SiO_2 scales on Si_3N_4 only. This focus is then on the associated equilibrium at the SiO_2/Si_2N_2O interface. The parabolic rate constant for Si_3N_4 is about 10^{-2} that of silicon at 1600 K, and, thus,

$$k_p(\text{Si}) = 10^2(k_p(\text{Si}_3\text{N}_4)) \tag{10}$$

$$2DK\Delta P_{O_2}^{\text{Si}}/N_O = 10^2\, 2DK\Delta P_{O_2}^{\text{Si}_3\text{N}_4}/N_O \tag{11}$$

where D is the diffusivity of oxygen in SiO_2, K a proportionality constant relating pressure to concentration, ΔP_{O_2} the pressure difference through the SiO_2 scale on the designated substrate, and N_O the number of oxygen atoms incorporated into the scale. All the constants, including D, cancel, and

$$\Delta P_{O_2}^{\text{Si}} = 10^2 \Delta P_{O_2}^{\text{Si}_3\text{N}_4} \tag{12}$$

Because the oxidation of silicon fits well with known diffusion coefficients, the pressure at the oxide/silicon interface is set by the SiO_2/Si equilibrium and can be taken as zero. Thus,

$$\Delta P_{O_2}^{Si} = P_{g,O_2} = 10^2(P_{g,O_2} - P_{i,O_2}^{Si_3N_4}) \quad (13)$$

If P_{g,O_2} is taken as 1, then $P_{i,O_2}^{Si_3N_4}$ is about 0.99 bar. A condition for diffusion control is thermodynamic equilibrium at the SiO_2/Si_2N_2O interface:

$$Si_2N_2O + 1.5O_2 = 2SiO_2 + N_2 \quad (14)$$

Putting a value of 0.99 bar for P_{O_2} into the equilibrium constant for this equation gives a nitrogen pressure of 10^{24} bar at 1600 K, an impossibly high value. There are three possible explanations for this: (1) thermodynamic equilibrium is not attained at the interface, (2) SiO_2 scale formed on Si_3N_4 may be different from that formed on silicon, and (3) network exchange diffusion may occur in the Si_3N_4 case at the same temperature at which molecular oxygen diffusion occurs in the silicon case. If the first is true, diffusion cannot be truly rate controlling. This supports some type of mixed control, which has been suggested by Luthra.[38,58] There is no clear evidence of a different type of SiO_2 scale being formed on Si_3N_4 than on silicon. Some investigators have suggested that nitrogen or nitrogen compounds diffusing outward may create some sort of blocking effect to oxygen diffusion inward,[54] but this is difficult to prove experimentally. If nitrogen has such an effect, one would expect a dependence of the rate on P_{N_2}, which has not been observed.[9] Double oxidation experiments support molecular oxygen diffusion for both silicon and Si_3N_4, discounting the third explanation.[56]

Luthra[58] has reconciled these differences by suggesting rate control by mixed interfacial reaction and nitrogen diffusion outward. He replots the data of Du *et al.*[9] on a plot of logarithm of thickness versus logarithm of time. Assuming that the growth rate obeys the parabolic portion of Eq. (1), the slope of such a plot should be 0.5. However, the slope is 0.96 at 1373 K and 0.70 at 1673 K.[58] This suggests a transition from interfacial reaction control through mixed interfacial reaction and diffusion control. The inclusion of interfacial reaction control may also explain the differences between silicon, SiC, and Si_3N_4, since the interfacial reaction is different for these systems.

Du *et al.*[9,57] have explained the differences between SiC and Si_3N_4 on the basis of duplex layer formation on Si_3N_4. Figure 12 is a cross section of oxidized Si_3N_4 which shows the duplex scale of Si_2N_2O and SiO_2. The stoichiometry of the oxynitride is most likely a solid solution, but it is generally identified as Si_2N_2O. In general, the thickness ratio of oxide to oxynitride is on average about 9 to 1.[9] Du *et al.*[9,57] have proposed that oxygen diffusion inward is rate controlling and that this Si_2N_2O layer has a lower permeability to oxygen than SiO_2 and thus acts as a diffusion barrier. Ogbuji[59] has recently performed experiments oxidizing Si_3N_4 and SiC at 1573 K and then annealing in argon at 1773 K and reoxidizing at 1573 K. In the first oxidation the rates of Si_3N_4 are much slower than those of SiC. However, the annealing removes the Si_2N_2O layer and the two rates become comparable. This supports the concept of Si_2N_2O as a barrier to oxygen diffusion inward. But the inconsistencies for rate control by oxygen diffusion inward still remain.

In summary, a fundamental understanding of SiC and Si_3N_4 oxidation is emerging, but many questions are unanswered. These deal with the rate-controlling step and the transport mechanism through SiO_2 scales. The differences between SiC and Si_3N_4, which are apparent for short oxidation times and below 1700 K, continue to be an intriguing problem.

V. Isothermal Oxidation—Additive-Containing Materials

The discussion thus far has centered on highly pure materials oxidizing in pure oxygen for short times and forming amorphous SiO_2. The situation in actual combustion environments is more complex. First, consider isothermal oxidation on less-pure materials. In a combustion situation the amorphous scale

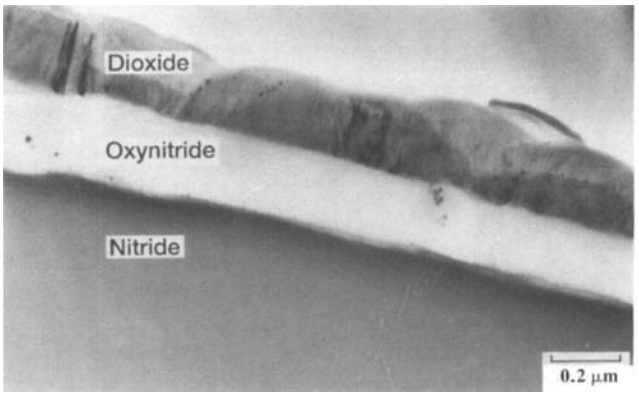

Fig. 12. Cross section of Si_3N_4 oxidized for 48 h at 1673 K, showing Si_2N_2O layer. The SiO_2 layer has been thinned. (Courtesy of L. Ogbuji, NASA Lewis.)

may often crystallize because of impurities in the substrate or water in the environment. Figure 13 shows a micrograph of spherulitic cristobalite forming on SiC. In general, transport in cristobalite is slower than transport in amorphous SiO_2. Costello and Tressler[42] have correlated a slowing of reaction rates with crystallization of the oxide scale. The exact nature of crystallization is highly dependent on impurities in the specimen and/or the atmosphere. However, for sintered α-SiC with boron and carbon additives, crystallization begins at the SiO_2/SiC interface and spreads to the surface.[23,60]

Densification aids in SiC and Si_3N_4 have an even more complex effect. The refractory oxide additives, such as magnesium oxide (MgO), alumina (Al_2O_3), and yttria (Y_2O_3), tend to migrate out to the SiO_2 scale and form the corresponding silicate.[61-74] Figure 14 is a sample of Y_2O_3-containing Si_3N_4 oxidized for 100 h. The bright, acicular crystallites at the surface are an yttria-silicate. Clarke[73] has reported that two forces drive these transition metals to diffuse to the surface. The additives are initially present as a grain-boundary silicate glass. The initially pure SiO_2 layer creates a gradient and a driving force for the cations to diffuse into this glass. The free energy of silicate formation in the surface SiO_2 is a second driving force.

In the case of SiC hot-pressed with Al_2O_3, an observed pressure dependence on oxygen[66] suggests that oxygen diffusion inward is still the rate-controlling step. However, enough aluminum diffuses into the scale to form an aluminosilicate.[42,61,62,66] Generally, this phase appears to accelerate rates.[42,62] In the case of SiC sintered with boron and carbon sintering aids, boron diffuses into the scale.[67] It creates a lower viscosity scale, which leads to somewhat higher oxidation rates

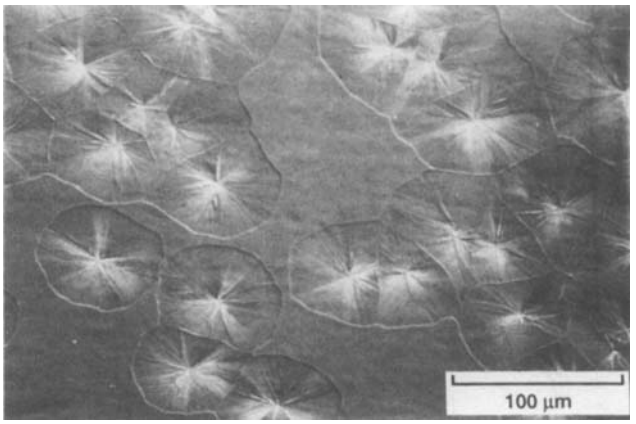

Fig. 13. Micrograph of SiC oxidized for 24 h at 1673 K, showing formation of spherulitic cristobalite. (Courtesy of E. Opila, NASA Lewis.)

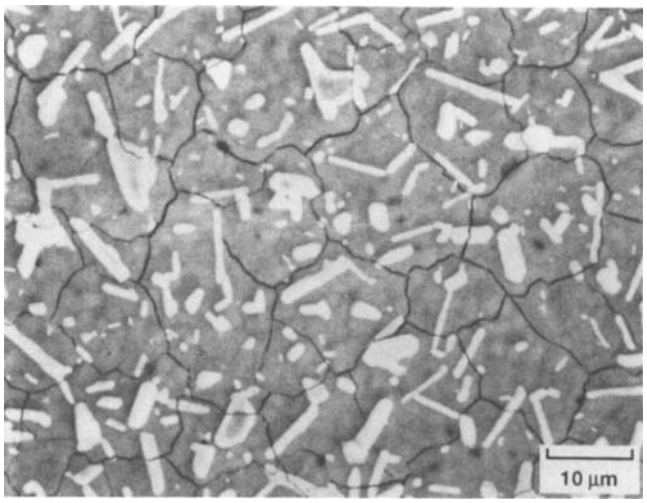

Fig. 14. Crystalline yttria silicate formed by migration of yttria impurities into scale.

over pure SiC. It has also been suggested that the formation of boron hydroxide is responsible for the bubbling from oxidation observed in this material.[40] The high thermodynamic stability of boron hydroxide indicates it can form at substantial pressures with a small pressure of water vapor and small amount of boron.

In the case of hot-pressed Si_3N_4 with MgO and Y_2O_3 additives, Singhal[64] and Cubicciotti and Lau[69] have seen no pressure dependence on oxygen. This differs from the observations for CVD Si_3N_4 (Ref. 9) and indicates another oxidation mechanism. Cubicciotti and Lau[68,69] have performed reoxidation experiments on MgO- and Y_2O_3-containing Si_3N_4. Here they oxidized for a time interval, polished the scale off, and reoxidized. They found that the process simply continues, as shown in Fig. 15. From this and microprobe data they concluded that the oxidation is controlled by migration of the magnesium or yttrium cations outward through the grain-boundary phase. More recently, Andrews and Riley[71] have shown that both cation outward diffusion and oxygen inward diffusion are important for some types of Si_3N_4.

These additives can have other effects on oxidation. In some cases liquid silicates may form.[65] It has been shown that oxidation rates increase with the amount of additives[62] and that additives lead to deviations from the parabolic rate law.[70] Also note

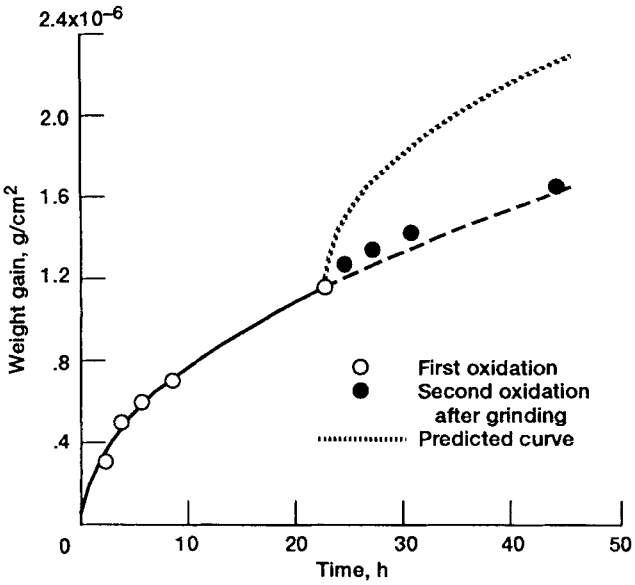

Fig. 15. Reoxidation curve for Si_3N_4 with MgO additives.[68]

that certain compositions of a Y_2O_3-containing Si_3N_4 have been found to catastrophically oxidize at 1273 K. This has been found to be due to the oxidation of a grain-boundary phase and the associated volume expansion.[75] The surface oxide does not form in a sufficient quantity to protect the grain boundaries at 1273 K.

Related to this is the oxidation of porous SiC and Si_3N_4 materials. There are several studies on reaction-sintered Si_3N_4, which is about 15% porous.[76,77] In general, these studies show that internal oxidation of the pores is critical. Porz and Thummler[77] have shown that the oxidation of Si_3N_4 at the pore mouth tends to limit the diffusive flow of oxygen into the interior of the Si_3N_4. Thus, material with small pores can show good oxidation behavior. Also, a preoxidation at high temperatures may limit oxygen penetration.

VI. Long-Term Oxidation and Thermal-Cycling Effects

The studies discussed to this point deal with short-term, laboratory-scale studies, typically on the order of several hours. In a heat exchanger or utility turbine a component may be subjected to isothermal conditions for hundreds or thousands of hours. Information on the effects of these long-term exposures is limited. Events such as crystallization may tend to slow reaction rates over initial rates obtained from amorphous scales. Some 500- to 1000-h tests in complex CO_2 and H_2O environments indicate that parabolic rates hold for these long times.[78,79] Fox[80] has shown that, after 100-h isothermal oxidation of SiC in oxygen, the calculated parabolic rate constants are in reasonable agreement with those extrapolated from several-hour exposures. His studies on CVD Si_3N_4 also indicate that the short-term rates may not extrapolate and that the long-term rates are close to those for CVD SiC, even below 1700 K.[80] The reasons for this are not clear.

Many long-term applications, such as an aircraft turbine or an internal combustion engine, involve thermal cycling. For this reason extensive studies have been done on cyclic oxidation of metal alloys.[81] However, studies on the cyclic oxidation of silicon-based ceramics are limited. SiO_2 undergoes a number of phase transformations on heating and cooling. Figure 16 shows the thermal expansivity for polycrystalline SiC, amorphous SiO_2, and crystalline SiO_2.[82] This mismatch between the coefficients of thermal expansion of the substrate and the scale may lead to tensile stresses and cracking. Figure 14 illustrates scale cracking. The question is to assess the effect of this cracking on oxidation rates.

The limited studies on cyclic oxidation indicate that SiC and Si_3N_4 perform relatively well under thermal cycling. Figure 17 shows a kinetic curve for sintered α-SiC containing carbon and boron additives tested at cycles of 5 h at 1773 K in air and then cooling to room temperature.[83] Also shown is a curve for isothermal oxidation. The two tests show very similar behavior. Similar results have been obtained at 1573 K. It appears that any cracks induced by the cycling heal immediately at these temperatures and scale thicknesses. Further studies are underway for longer times.[83]

Lindberg[84,85] has examined a variety of commercial SiC and Si_3N_4 materials in a burner rig with 12-min cycles at 1643 K for a total of 3500 h. Durability was assessed from retained strength. In general, the dense, uniform-grain-size materials showed negligible strength reduction. Maeda *et al.*[86] have studied a sintered Al_2O_3-containing SiC for periods up to 3000 h. Weight gains were comparable to those obtained during isothermal oxidation, but the actual kinetics involved at least four different parabolic stages. They attribute these to the various microstructural changes in the scale: crystallization of amorphous silica, transformation of those crystalline phases, and viscosity changes in the oxide scale due to migration of the additives. In the early stages a smooth scale is formed following parabolic kinetics; as time progresses, cracks and bubbles develop, leading to more rapid rates, and then these heal over leading to slower rates. Andrews and Riley[87] have studied a

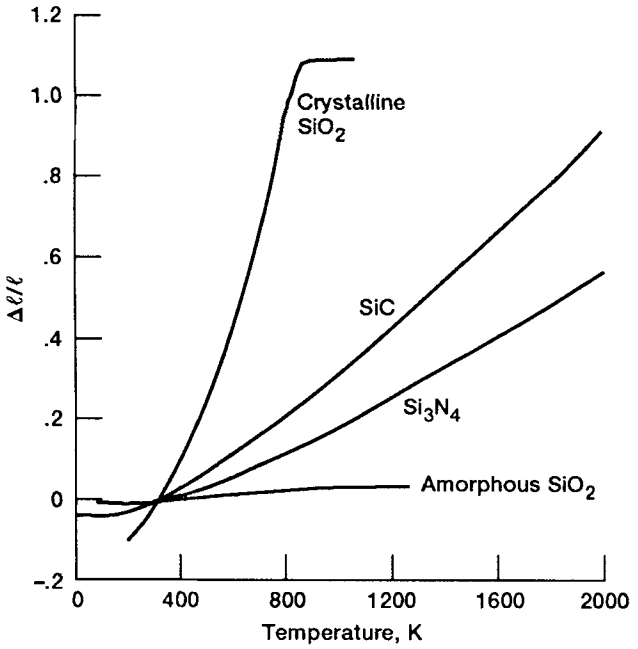

Fig. 16. Thermal expansion of SiC, Si_3N_4, amorphous SiO_2, and crystalline SiO_2 as a function of temperature.[82]

Si_3N_4 containing various oxide additives. Again the strength shows relatively little change. Weight gains are similar to isothermal oxidation, although again the kinetics are somewhat different. Some of these differences may be attributed to scale cracking on cycling.

VII. Isothermal Oxidation—Carbon Dioxide and Water as Oxidants

Actual combustion atmospheres are not simply pure oxygen. All combustion environments contain nitrogen, CO_2, and H_2O. Fuel-lean environments contain oxygen; fuel-rich environments contain CO and hydrogen. Thus, the primary oxidant

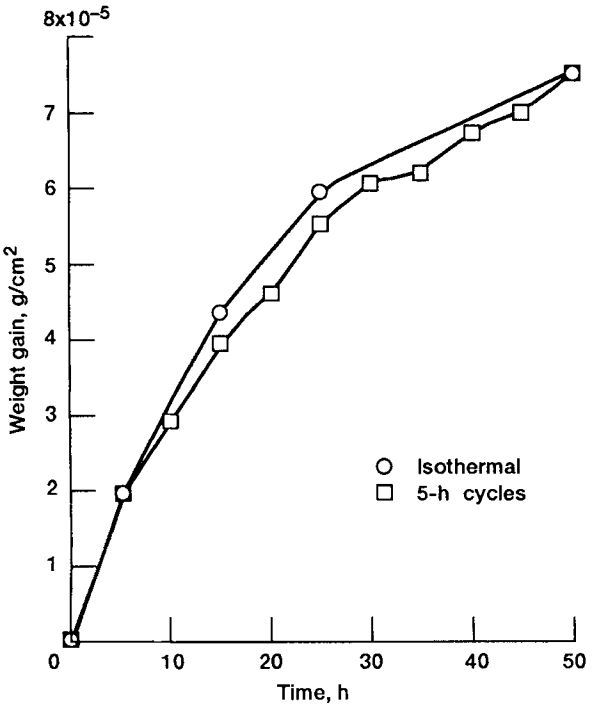

Fig. 17. Cyclic oxidation curve for sintered α-SiC with carbon and boron additives at 1773 K, 5-h cycles.

may not always be oxygen; it may also be H_2O and CO_2. H_2O may induce crystallization and thereby change oxidation behavior. It may also alter transport properties through the scale.

Consider first the effect of H_2O on isothermal oxidation of pure silicon. Deal and Grove[31] have shown that silicon oxidizes over an order of magnitude faster in wet oxygen than in dry oxygen. They attribute this to the higher solubility of H_2O in SiO_2 ($\sim 3.4 \times 10^{19}$ molecules/cm^3) versus molecular oxygen in SiO_2 ($\sim 5.5 \times 10^{16}$ molecules/cm^3).[31,88] As Eq. (2) shows, the parabolic rate constant is directly proportional to the solubility of the oxidizing species. Deal and Grove further show that silicon oxidizes at the same rate regardless of whether the mixture is H_2O/Ar or H_2O/O_2. This indicates that H_2O is the primary oxidizing species. Irene and Ghez[89] have further shown that H_2O disrupts the SiO_2 network by forming nonbridging SiOH groups. This modified SiO_2 network permits faster H_2O transport.

One would expect similar behavior for SiC. There is general agreement that H_2O accelerates the oxidation of SiC.[45,63,90–94] The major reaction is very likely

$$SiC + 3H_2O(g) = SiO_2(s) + CO(g) + 3H_2(g) \quad (15)$$

Jorgensen *et al.*[90] have studied the oxidation of SiC powders and found the rates to be proportional to log P_{H_2O}. Cappelen *et al.*[91] have observed that the rate in H_2O/N_2 and H_2O/O_2 is the same, indicating that, as in pure silicon, the primary oxidizing species is H_2O. They also have observed parabolic rates in pure oxygen and linear rates in H_2O. It appears that H_2O diffusion is so rapid that the rate-controlling step becomes the interfacial reaction. Narushima *et al.*[92] have studied SiC in wet oxygen for longer times and observed an initial linear region followed by a parabolic region. Unlike oxidation in dry oxygen, the linear region lasts long enough ($\sim$1 h) to measure reliable linear rate constants. Apparently the rapid permeation of H_2O extends the period of interfacial reaction control. Tressler *et al.*[94] have examined the effect of water vapor on the oxidation of single-crystal SiC and sintered α-SiC. In both cases steam accelerated oxidation by about 10 to 20 times, which is attributed to more rapid permeation of the H_2O molecules, very likely by incorporation of $(OH)^-$ into the SiO_2. Recent work in purified oxygen versus 10% water vapor/purified oxygen has shown an increase in the parabolic rate constant by a factor of 2 to 3 at 1473 K.[45] Particular care was taken to avoid the effects of sodium impurities, which may often effect this type of measurement.[45,54] There are some important questions on the effects of water vapor on SiC oxidation.

Choi *et al.*[54] have examined the oxidation of Si_3N_4 in wet oxygen. They have observed somewhat different behavior than for wet oxidation of silicon or SiC. In the case of H_2O/Ar, the pressure of H_2O has no effect on the rates. However, in the case of H_2O/O_2 the rates show a complex dependence on P_{H_2O}. They attribute the wet oxidation to the following reactions:

$$Si_3N_4(s) + 6H_2O(g) = 3SiO_2(s) + 4NH_3(g) \quad (16)$$

$$4NH_3(g) + 5O_2(g) = 6H_2O(g) + 4NO(g) \quad (17)$$

They suggest that the effects of H_2O on Si_3N_4 oxidation are due to the product (NH_3 and NO) gases blocking the outward diffusion paths, increased solubility of H_2O versus molecular oxygen in SiO_2, or different adsorption properties of gaseous molecular oxygen versus water vapor.

In addition to water vapor, CO_2 may act as an oxidant in a combustion environment. Antill and Warburton[78] have studied long-term oxidation of SiC in CO_2. They generally saw parabolic behavior and rates about an order of magnitude slower than those in pure oxygen. Warburton *et al.*[79] have also examined long-term oxidation of porous Si_3N_4 containing MgO. Parabolic behavior was generally observed, although the sealing off of internal porosity in this material was a critical factor.

In summary, many questions remain about the effect of water vapor and CO_2 on the oxidation of SiC and Si_3N_4. It is accepted that water vapor induces devitrification in SiO_2 scales and

accelerates the oxidation of SiC. The differences between SiC and Si_3N_4 are still not understood.

VIII. Combustion Environment Impurity Effects

In addition to the various gases shown in Fig. 3(a), combustion environments may also contain a number of corrosive impurities. These include sulfur oxides SO_2 and SO_3, carbon-containing gases, hydrogen chloride (HCl), sodium, vanadate compounds, and transition-metal atoms. Even in small quantities these impurities may have a deleterious effect on a silicon-based ceramic.

In most combustion environments sulfur is present as SO_2 and SO_3, and, thus, the environment is oxidizing–sulfidizing. It has been shown that pure SiO_2 is resistant to attack by SO_2 and SO_3.[95] Limited experiments by the author have shown that exposure to SO_2 has no measurable effect on SiC at 1473 K over several hours. In some coal combustion situations, it may be possible to obtain more sulfidizing environments because of the presence of hydrogen sulfide (H_2S) and low oxygen potentials. Under these conditions a stable SiO_2 scale may not form, and formation of $SiS(g)$ and $SiO(g)$ may lead to rapid degradation.[96,97]

The major carbon-containing species are CO and CO_2, so that the combustion environment is also oxidizing–carburizing. CO_2 is an oxidant, and its behavior has been discussed. $SiO(g)$ forms in predominantly CO environments, as discussed in more detail in the next section. Actual combustion environments contain a mixture of these impurities, generally with sufficient CO_2 to be oxidizing. In some coal combustion situations there may be a high carbon activity and a low oxygen activity. Where hydrocarbons such as methane are present, a net transport of SiC has been observed.[96] The low oxygen potential allows $SiO(g)$ to be formed, and it subsequently reacts as

$$SiO(g) + CH_4(g) = SiC(s) + H_2O(g) + H_2(g) \qquad (18)$$

Such a route leads to rapid degradation.

Chlorine corrosion can be an issue due to the formation of the stable $SiCl_x$ species.[98,99] In general, chlorine can be quite reactive with SiC in a low-P_{O_2} environment. In a heavily oxidizing environment, it has been found that 5% Cl_2/O_2 environments show enhanced oxidation by a factor of 10 over pure oxygen. This has been attributed to incorporation of chlorine in the SiO_2 network and the subsequent formation of nonbridging bonds leading to a more open structure.[100] It is more likely that HCl will form in combustion environments. Short-term exposures of SiC to HCl/O_2 mixtures show no major effects.[98]

Alkali metals (sodium and potassium) are common impurities in heat engines and industrial furnaces. These impurities may be present in the fuel, in the intake air in a marine environment, or as a byproduct of an industrial furnace, such as an aluminum remelt furnace. Most alkali-induced corrosion is due to large deposits of Na_2SO_4 forming on the material, as discussed in a subsequent section. However, there are some recent studies of very-low-level sodium and potassium incorporation into a growing SiO_2 scale on SiC. Such a situation is possible in combustion environments and provides some insights into the mechanism of modified SiO_2 growth in the presence of impurities.

Pareek and Shores[101] have studied the oxidation of SiC with carefully controlled amounts of potassium. Basically, they have used potassium carbonate (K_2CO_3) as their source of potassium and have controlled the activity by varying the P_{H_2O} to P_{CO_2} ratio:

$$K_2CO_3 + H_2O = 2KOH + CO_2 \qquad (19)$$

For dry CO_2/O_2 mixtures, which lead to a very small amount of potassium incorporated into the scale, they observe enhanced parabolic oxidation. They attribute this to potassium modification of the SiO_2 network. For CO_2–O_2–H_2O mixtures they observe linear rate laws that they suggest are due to the rapid transport of H_2O through the scale. Zheng *et al.*[102,103] have made similar observations for SiC and Si_3N_4 at 1373 to 1573 K. In their case, sodium is ion implanted into the SiC sample. Thus, the concentration of sodium in the growing SiO_2 scale remains constant. The same oxidation mechanism is maintained, but faster rates are observed. For SiC they attribute an increase of oxidation by a factor of 2 to the formation of nonbridging oxygens, which allows faster molecular diffusion through the SiO_2 scale. For Si_3N_4 the situation is less clear, but they attribute the acceleration of oxidation rates by a factor of 14 to a modification of the Si_2N_2O layer.

In addition to sodium, transition metals, such as vanadium, iron, nickel, and chromium, may also be present from the fuel and/or the metallic parts of the engine or furnace. These too may be incorporated into the scale, leading to enhanced oxidation.

In the case of metals, small amounts of impurities can lead to severe corrosion. In general, this information is lacking for ceramics. Current evidence suggests that, in oxidizing environments, the stable SiO_2 scale prevents extensive attack from gaseous impurities. However, metal-atom impurities may be incorporated into the scale and lead to more rapid oxidation.

An actual burner rig test encompasses oxidation in the presence of impurities and thermal cycling. These burner rigs thus provide the most realistic test. In general, SiC and Si_3N_4 have shown good durability in fuel-lean environments to about 1673 K.[104,105] Significant effects noted in these studies include the incorporation of metal impurities in the SiO_2 scale from the metallic parts of the burner rig and the deformation of the SiO_2 scale due to the high velocity of the burner rig. Scales of lower viscosity, such as those grown on additive-containing SiC and Si_3N_4, tend to deform more than a pure SiO_2 scale.

IX. Volatility Issues and Active Oxidation

(1) Silicon Dioxide Scale Volatility

As Fig. 4 shows, two major degradation routes are scale volatility and active oxidation to $SiO(g)$. Consider first the volatility of the SiO_2 scales. The vapor species above SiO_2 are most conveniently represented by a volatility diagram, as shown in Fig. 18. These diagrams have a variety of applications and have been discussed by a number of investigators.[97,106–108] Note that, at 1-bar oxygen pressure, the major vapor species above SiO_2 is $SiO_2(g)$ and the minor species is $SiO(g)$.

In a combustion situation the question to address is how much material will be lost by vaporization into the flowing gas stream. It can be shown that the flux of gas vaporizing through a boundary layer into a flowing gas stream is given by[109,110]

$$J = \frac{\alpha P^{eq}_{SiO_x}/(2\pi MRT)^{1/2}}{1 + \alpha P_t/[(2\pi MRT)^{1/2}h_m]} \qquad (20)$$

where α is the sticking coefficient, $P^{eq}_{SiO_x}$ the equilibrium vapor pressure of $SiO_x(g)$ in the atmosphere of interest, M the molecular weight of SiO_x, R the gas constant, T the temperature in degrees Kelvin, P_t the total pressure, and h_m the mass transport coefficient. Note that Eq. (20) has the correct limits. For low pressures or fast velocities (large h_m), $\alpha P_t/[(2\pi MRT)^{1/2}h_m] << 1$, and the expression reduces to the Langmuir equation for vaporization into a vacuum. For high pressures or slower velocities, $\alpha P_t/[(2\pi MRT)^{1/2}h_m] >> 1$, and the expression is dominated by the mass transport coefficient. Under these conditions, α becomes unimportant, which is consistent since α has meaning only in a low-pressure situation.

The mass transport coefficient can be derived from various semiempirical correlations. Consider, for example, a combustion chamber modeled as a hollow cylinder, with vaporizing walls:[111]

$$h_m = (0.026D_{SiO_x}/RTLP_t)\,(\nu/\rho D_{SiO_x})^{0.33}(\rho vL/\nu)^{0.8} \qquad (21)$$

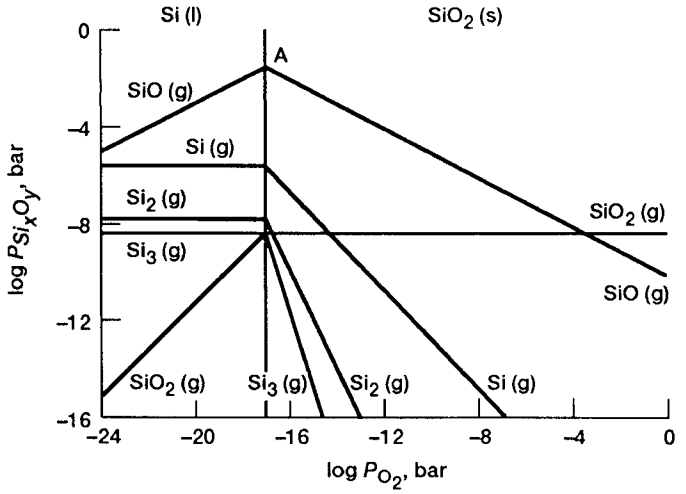

Fig. 18. Volatility diagram for the Si–O system at 1800 K. (From Kohl *et al.*[107])

where D_{SiO_x} is the diffusion coefficient of SiO_x in the combustion atmosphere, L a characteristic dimension taken to be the diameter of the cylinder, ν the viscosity of the combustion gas, ρ the density of the combustion gas, and $\mathbf{v}$ the linear gas velocity. From Eqs. (20) and (21) one can extract a relationship between flux and vapor pressure. Note that this is only an approximation because many of the terms in Eq. (20) are temperature dependent. However, because vapor pressure shows an exponential temperature dependence and the other terms show fractional power temperature dependence, this is a reasonable approximation.

The issue then is to determine an acceptable flux and thereby extract an acceptable vapor pressure limit. An acceptable flux depends on the application. For clarity, flux can be converted to recession rate as follows:

$$R(\text{m/s}) = 10^{-6}J(\text{mol/(m}^2\cdot\text{s)})\text{MW}/\rho' \qquad (22)$$

where MW is the molecular weight of SiO_2 and ρ' the density of SiO_2. There are no guidelines for acceptable recession rates; however, lifetimes of 10000 h or longer are desired for future combustor liners. This suggests a criterion of 10×10^{-3} in./10000 h, or 7.0×10^{-12} m/s. This in turn leads to a maximum acceptable vapor pressure of 10^{-6} bar as determined from Eqs. (21) and (22) and some approximate combustion chamber parameters. Other investigators have taken similar criterion.[112]

To determine when SiO_2 vaporization is a problem, one needs to know at what temperature the total pressure of the vapor species above SiO_2 is 10^{-6} bar. There are several equivalent ways to do this. First, for a simple overpressure of oxygen, one can read the total pressure from the volatility diagram for a range of temperatures. Second, one can solve the vaporization equations:

$$SiO_2(s) = SiO_2(g) \qquad K_p = P_{SiO_2} \qquad (23)$$

$$SiO_2(s) = SiO(g) + 0.5O_2(g) \qquad K_p = P_{SiO}(P_{O_2})^{1/2} \qquad (24)$$

$$O_2(g) = 2O(g) \qquad K_p = P_O^2/P_{O_2} \qquad (25)$$

An oxygen pressure can be put into the equilibrium constants of Eqs. (24) and (25), and then the three equations can be solved. Third, which is perhaps the most versatile, is to use a free-energy-minimization computer code[17,113] for determining the equilibrium vapor pressures. Basically, such a code takes solid SiO_2 and a particular combustion atmosphere and minimizes the total free energy of the system subject to certain constraints. The results are the equilibrium vapor pressures in that combustion atmosphere. The versatility of this approach is that volatility can be assessed in any combustion environment.

Figure 19(a) shows the vapor pressure above SiO_2 in a fuel-lean environment. These results are basically the same as the pressures taken from the volatility diagram (Fig. 18) at high oxygen potentials. Figure 19(a) shows that the pressure of SiO_2 approaches 10^{-6} bar only at temperatures near the melting point. Thus, vaporization in a fuel-lean environment is unlikely to be a major issue.

Figure 19(b) shows the vapor pressure above SiO_2 in an equilibrium fuel-rich environment. Note that now there is a substantial pressure of $SiO(g)$. A stable SiO_2 film is expected to form because of the oxidants CO_2 and H_2O. However, the source of $SiO(g)$ is reduction of SiO_2 in this environment. The higher total vapor pressures indicate that vaporization may be an issue at temperatures above 1770 K. It may be that, in a fuel-rich situation, coupled oxidation and vaporization lead to paralinear kinetics.[110,114]

(2) Active Oxidation

The most common route of $SiO(g)$ generation is active oxidation. Although this can lead to rapid degradation, it only occurs at low oxygen potentials. Most of the combustion environments are oxidizing with large amounts of the oxidants, molecular oxygen, CO_2, and H_2O. However, in some special cases, such as coal combustion, the oxidant pressure may fall below that needed for a stable SiO_2 film to form. In this case active oxidation would be favored:

$$Si + 0.5O_2 = SiO(g) \qquad (26)$$

$$SiC + O_2 = SiO(g) + CO(g) \qquad (27)$$

$$Si_3N_4 + 1.5O_2 = 3SiO(g) + 2N_2(g) \qquad (28)$$

In these cases a protective oxide film is not formed and the volatile products may lead to rapid consumption of the ceramic.

The major issue with active oxidation is the P_{O_2} transition point. Again, it is appropriate to begin with pure silicon. Heuer and Lou[108] show how volatility diagrams can be used to predict the active-to-passive transition. The P_{SiO} for a stable SiO_2 film can be determined from the necessary equilibrium

$$SiO_2(s) + Si(s) = 2SiO(g) \qquad (29)$$

This can be read from point A on the volatility diagram (Fig. 18) to be about 10^{-2} bar at 1800 K. Basically, enough oxygen to form 10^{-2}-bar $SiO(g)$ from Eq. (26) is required, which is 0.5×10^{-2}-bar oxygen. The factor of 0.5 is from the stoichiometry of Eq. (26). Therefore, the condition for the active-to-passive transition is

$$P_{O_2} = 0.5P_{SiO}^{eq} \qquad (30)$$

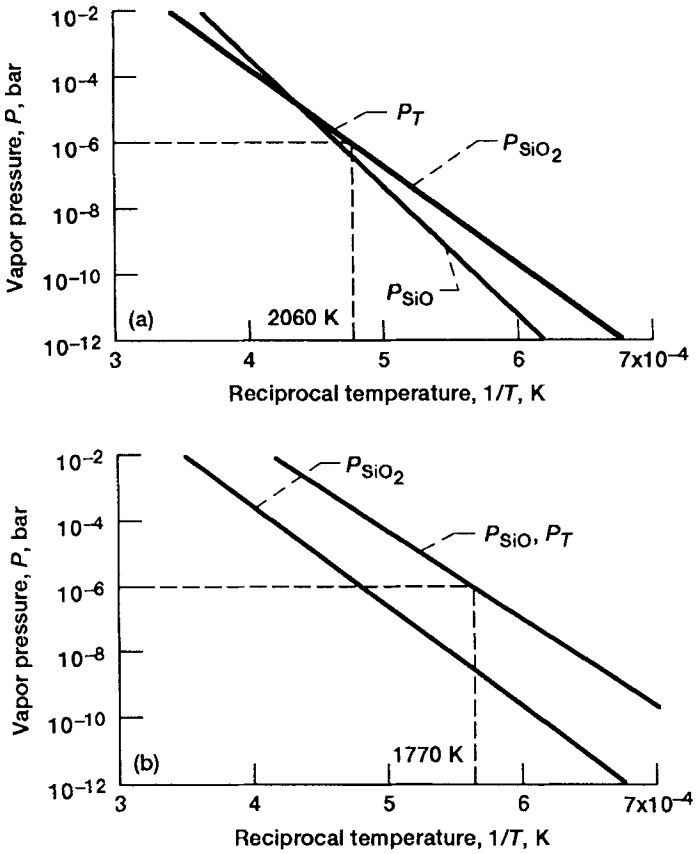

Fig. 19. Partial pressures of major vapor species in combustion atmospheres with Jet A fuel: (a) fuel-lean atmosphere, equivalence ratio of 0.5, $P_{O_2} = 0.10$ bar and (b) fuel-rich atmosphere, equivalence ratio of 1.75, $P_{O_2} = 5 \times 10^{-8}$ bar.

As P_{O_2} is increased above the active-to-passive transition point, SiO_2 first forms as a "smoke":

$$SiO(g) + 0.5O_2(g) = SiO_2(smoke) \quad (31)$$

This approach is similar to that of Turkdogan *et al.*[115] and is shown schematically in Fig. 20(a).

As Heuer and Lou[108] have reported, mass transport considerations are involved in this transition. Hinze and Graham[116] have reported that it is important to specify whether the low P_{O_2} is attained by lowering the total pressure (molecular flow regime) or by lowering P_{O_2} (viscous flow regime).

In a combustion situation, oxidant pressures are part of a high total pressure and the flow is in the viscous regime. The classic work in this area is by Wagner.[117] He has considered a silicon sample in contact with an O_2/He mixture. At very low P_{O_2}, SiO forms according to Eq. (26). To form a stable SiO_2 scale, enough $SiO(g)$ must be formed to maintain the equilibrium in Eq. (29). The transition P_{O_2} is the P_{O_2} necessary to form that amount of $SiO(g)$. This is a transport problem and depends on the diffusion of oxygen and SiO through the boundary layer. Solving this problem leads to the following relationship:

$$P_{O_2}^{trans} = 0.5(D(SiO)/D(O_2))^{1/2} P_{SiO}^{eq} \quad (32)$$

The diffusion coefficients can be estimated, and the expression reduces to

$$P_{O_2}^{trans} = 0.64 P_{SiO}^{eq} \quad (31)$$

This approach is shown schematically in Fig. 20(b). Note that this result is close to the results based on thermodynamic considerations alone, due to the fact that gas-phase diffusion coefficients are often close to unity.

The active-to-passive transition for SiC and Si_3N_4 is more complex because additional product gases form. A purely thermodynamic interpretation allows $P_{O_2}^{trans}$ to be determined from volatility diagrams as described by Heuer and Lou.[108] Singhal[118] has extended Wagner's theory and used the following analogues for Eq. (29) to derive a transition P_{O_2}:

$$SiC(s) + 2SiO_2(s) = 3SiO(g) + CO(g) \quad (34)$$

$$Si_3N_4(s) + 3SiO_2(s) = 6SiO(g) + 2N_2(g) \quad (35)$$

However, Hinze and Graham[116] have suggested that other equilibria may control this transition for SiC in place of Eq. (34):

$$SiC(s) + SiO_2(s) = 2SiO(g) + C(g) \quad (36)$$

$$2SiC(s) + SiO_2(s) = 3Si(l,s) + 2CO(g) \quad (37)$$

Their experimental data tend to support Eq. (37). This is similar to the result of Gulbransen and Jansson[106] for the transition

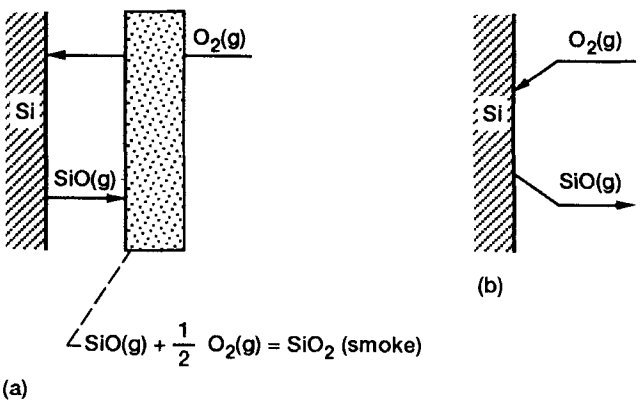

Fig. 20. Schematic of two proposed descriptions of active-to-passive transition for silicon: (a) thermodynamic considerations only, SiO_2 "smoke" formation, and (b) thermodynamic and mass transport considerations, Wagner theory.

in the molecular flow regime. Thus, the active-to-passive transition for SiC is given in terms of sufficient P_{O_2} to create enough CO to establish this equilibrium. Again using mass transport arguments similar to those of Wagner, they have derived the following expression:

$$P_{O_2}^{trans} = (D(CO)/D(O_2))^{1/2} P_{CO}^{eq} \quad (38)$$

Narushima *et al.*[119] have examined CVD SiC and come to a similar conclusion.

Nickel[120] has reported that carbon activity needs to be considered in establishing the active-to-passive transition. At high carbon activities the SiC/SiO_2 equilibrium is critical in establishing the transition. At low carbon activities Nickel proposes that the $SiO(l)/SiC$ equilibrium is important and thus the critical equilibria becomes

$$SiC(s) + SiO(l) = 2Si(l) + CO(g) \quad (39)$$

This approach fits some recent data quite well;[120] however, the existence of condensed-phase SiO is quite controversial.[121]

Numerous other studies of the active-to-passive transition have been performed. Antill and Warburton[122] have examined the transition in the presence of other oxidants (CO_2 and H_2O) and have found behavior similar to that in oxygen. This is important for a combustion environment, where the primary oxidants may be CO_2 and H_2O. Vaughn and Maahs[123] have shown that the P_{O_2} transition varies with flow rate, emphasizing the mass transport issue. The approximate active-to-passive oxidant transition pressures for SiC and Si_3N_4 are given in Fig. 4; more precise values are given in the references.[116–120,122,123]

In most combustion environments, active oxidation is not expected to be a problem. Combustors in current gas turbines burn near the stoichiometric region. The resultant environment contains oxygen, H_2O, and CO_2. Novel combustor designs may involve a fuel-rich region, which would contain CO, CO_2, H_2O, hydrogen, and oxygen potentials as low as about 10^{-9} bar (Fig. 3(a)). However, the presence of H_2O and CO_2 at about 0.1 bar each should form enough SiO to satisfy the equilibrium requirements for a stable SiO_2 scale (Eqs. (29) or (34) to (37) or (39), with H_2O and/or CO_2 as oxidants). The effect of water vapor in suppressing active oxidation has been discussed by Heuer and Lou.[108] Once formed, however, the SiO_2 scale may be reduced in the fuel-rich environment.

Thus, combustion of hydrocarbon fuels generally provides an atmosphere sufficient for forming SiO_2. However, coal combustion situations and certain heat-treating environments, which are heavily reducing, can lead to active oxidation. In a recent study of reactions of SiC in heat-treating environments, the kinetics of $SiO(g)$ formation are found to be dependent on the gas composition and additives in the ceramic.[124,125]

In summary, there are two causes of volatility. The first is SiO_2 vaporization. Unless the net SiO_x vapor pressure is greater than about 10^{-6} bar, this is not a major problem. In fuel-lean and stoichiometric combustion situations, this vapor pressure is attained near the melting point of SiO_2, so that volatility is not a limiting factor. In a fuel-rich situation, SiO_2 volatility is likely to be an issue at higher temperatures. The second cause of volatility is active oxidation. The key issue is the oxidant pressure for the active-to-passive transition. Active oxidation is predicted for only a limited number of combustion situations, and it can lead to rapid material consumption.

X. Upper Temperature Limits

Referring to the corrosion diagram (Fig. 4), the absolute upper use temperature for silicon-based ceramics is ~2000 K. This is the melting point of SiO_2. When the protective oxide is liquid, it begins to flow, and rapid transport rates are obtained. This is a nonprotective situation. Figure 21 shows a sample of SiC oxidized for 1 h in air at 2073 K. Note the extensive corrosion. The question then is how close to 2000 K can one safely use this material.

Several issues limit the use of SiC below 2000 K. These include rapid oxidation rates, volatilization of the SiO_2 film, and reaction of the SiO_2 film with the SiC or Si_3N_4 substrate. Oxidation and volatility have been discussed previously. Note that there are relatively few measurements at these high temperatures because it is difficult to attain such temperatures in oxidizing environments.

An important difference between silicon-based ceramics and other oxide-protected metal alloys is that, at sufficiently high temperatures, the oxide scale and the SiC or Si_3N_4 ceramic react. Such reactions can generate gas pressures at the oxide/ceramic interface:

$$SiC(s) + 2SiO_2(s) = 3SiO(g) + CO(g) \quad (40)$$

$$Si_2N_2O(s) + SiO_2(s) = 3SiO(g) + N_2(g) \quad (41)$$

The best way to examine these interfacial reactions is with the Si–C–O and Si–N–O predominance diagrams, which are shown in Fig. 22. The intersection of the SiO and CO isobars with the SiC/SiO_2 coexistence line (line AB) gives the gas pressures in the carbide system, as shown in Fig. 22(a). The intersection of the SiO and nitrogen isobars with the Si_2N_2O/SiO_2 coexistence line (line AB) gives the gas pressures in the nitride system, as shown in Fig. 22(b).

Consider first the Si–C–O system. Figure 23(a) shows these total pressures as a function of temperature for the carbon-saturated, stoichiometric, and silicon-saturated systems. Taking 1 atm as the criteria for instability, carbon-saturated SiC in contact with SiO_2 becomes unstable at 1800 K. Pressures approach 1 atm for the other systems near the melting point of SiO_2. These types of reactions have been suggested as the source of bubbling at very high temperatures in an oxidized SiC sample.[41,126]

Recently, Jacobson *et al.*[127] have examined the SiC + SiO_2 reaction in detail. They have found that a carbon-saturated system tends to adjust to a stoichiometric composition. This is done by releasing a large amount of CO and forming a secondary SiC. Such a process at the carbon-saturated SiC/SiO_2 interface may lead to extensive bubbling.

The Si–N–O system is more complex because two interfaces are involved. However, Eq. (41) is predicted to be the major source of $SiO(g)$ and $N_2(g)$. The total pressures are shown in Fig. 23(b). The pressures predicted are less than those in the Si–C–O system. This may be the reason that only limited bubbling is observed when Si_3N_4 is oxidized at high temperatures.[41]

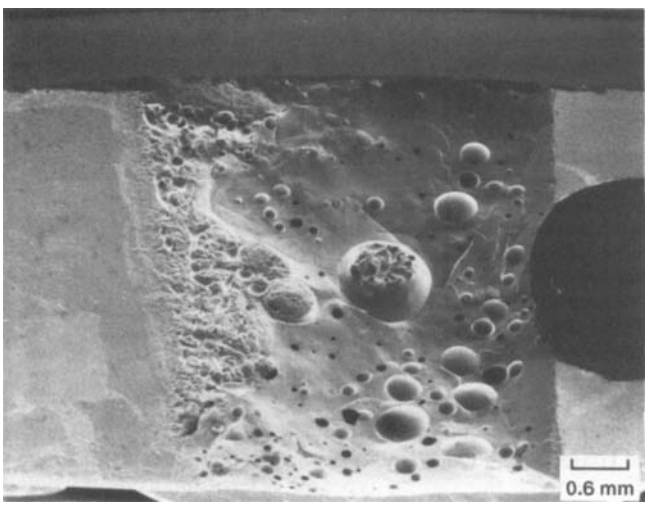

Fig. 21. Chemically-vapor-deposited SiC oxidized for 1 h at 2073 K in air. (Courtesy of D. Fox, NASA Lewis.)

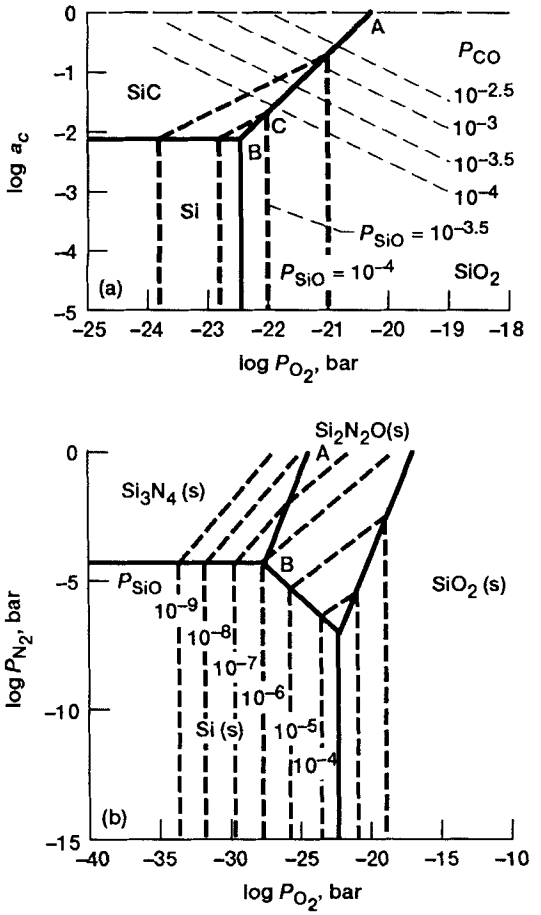

Fig. 22. Predominance diagrams at 1500 K: (a) Si–C–O system and (b) Si–N–O system.

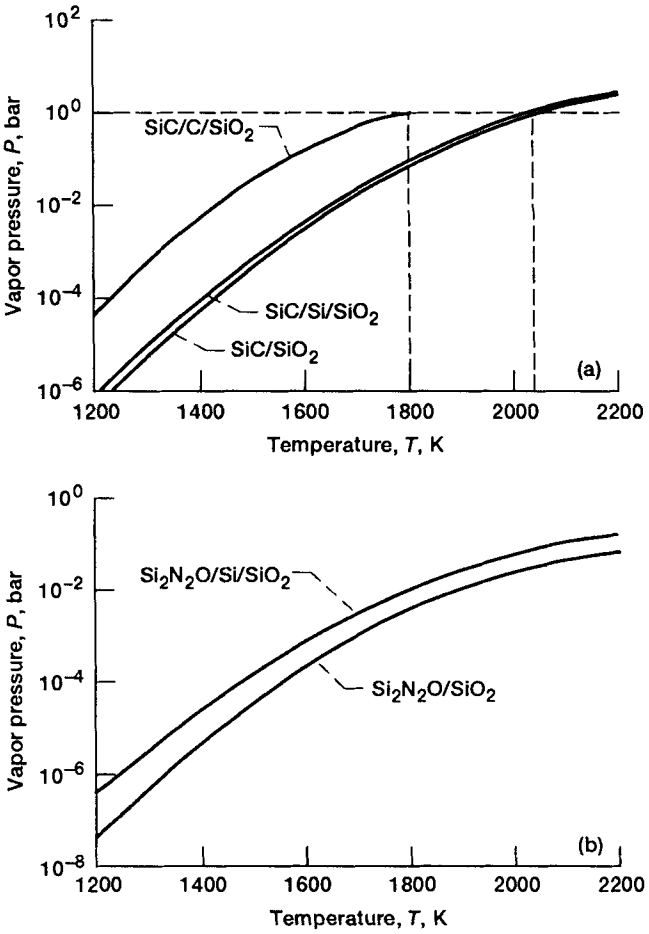

Fig. 23. Total vapor pressure at interfaces: (a) SiC/SiO_2 interface and (b) Si_2N_2O/SiO_2 interface.

In summary, the upper use temperatures of silicon-based ceramics are limited by scale melting, oxidation rates, volatility, and scale/substrate reaction. Scale melting occurs at 1996 K. Oxidation and scale volatility are highly dependent on ceramic composition and atmosphere. The scale/substrate reaction is more of an issue in SiC than in Si_3N_4.

XI. Deposit-Induced Corrosion

(1) Formation of Deposits

As discussed previously, dopant levels of sodium in SiO_2 scales appear to accelerate oxidation. Larger amounts of sodium, either from a marine environment, a salted roadway, or fuel impurities, can react with sulfur fuel impurities to form Na_2SO_4, which is a highly stable molecule:[18]

$$2NaCl(g) + SO_2(g) + 0.5O_2(g) + H_2O(g) = Na_2SO_4(l) + 2HCl(g) \quad (42)$$

The Na_2SO_4 forms as a deposit on engine parts. This type of deposit-induced corrosion is termed "hot corrosion," and there is a large amount of literature on hot corrosion of metals.[128,129] The studies on silicon-based ceramics have recently been summarized.[130]

The primary emphasis in this section is on Na_2SO_4-induced attack. However, there are other types of deposit-induced corrosion (e.g., vanadate-induced attack from lower purity fuels[131] and oxide-slag-induced attack from coal combustion[6]). Similarities between the various types of deposit-induced attack are discussed below.

In general, hot corrosion occurs in two steps: (1) deposition and (2) corrosive attack. It is first necessary to determine when a corrosive Na_2SO_4 deposit forms. Generally, Na_2SO_4 is corrosive between its melting point (1157 K) and the dewpoint for Na_2SO_4 deposition. The latter can be calculated from a free-energy-minimization computer code.[17] The dewpoints are shown in Fig. 24 for a number of different combustion conditions. These factors tend to limit the region of hot corrosion, as shown in Fig. 4. There are two issues to note from this. First, although the region is limited, it is important to be aware of hot corrosion because it can be quite severe. Second, the dewpoint tends to increase with pressure. Future engines are expected to operate at higher temperatures and pressures. Higher temperatures decrease the likelihood of deposition by exceeding the dewpoint; however, higher pressures will increase the dewpoint. Thus, a knowledge of engine operating parameters is essential for predicting the presence of a deposit.

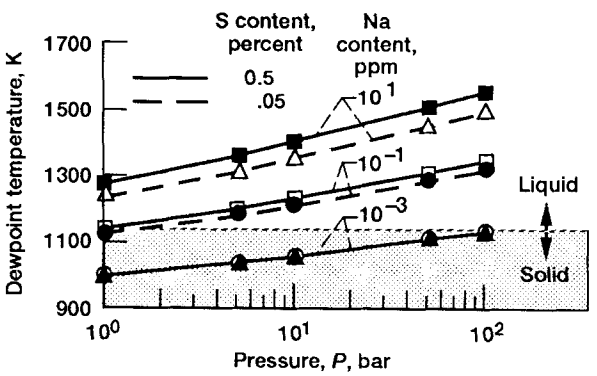

Fig. 24. Dewpoints for Na_2SO_4 deposition.

(2) Thermodynamics of Deposit-Induced Corrosion

Figure 25 shows a coupon of SiC treated in a burner rig both with and without added sodium.[132] Note the dramatic effect. Elemental maps of a polished cross section are shown in Fig. 26. Note the even distribution of sodium, oxygen, and silicon in the scale, suggesting the formation of sodium silicate glass. Sulfur was not detected in the scale, indicating that any deposited Na_2SO_4 had decomposed. The likely reaction scheme for this is

$$SiC(s) + 1.5O_2(g) = SiO_2(s) + CO(g) \quad (43)$$

$$xSiO_2(s) + Na_2SO_4(l) = Na_2O{\cdot}x(SiO_2)\ (l) + SO_3(g) \quad (44)$$

These are the key reactions in hot corrosion. A solid, protective SiO_2 scale has been converted to a liquid scale. Transport rates through the liquid are rapid, leading to accelerated attack.

Equation (44) can best be understood as an acid–base reaction.[18,128] It can be written more fundamentally as

$$Na_2SO_4(l) = Na_2O(s) + SO_3(g) \quad (45)$$

$$xSiO_2(s) + Na_2O(s) = Na_2O{\cdot}x(SiO_2)\ (l) \quad (46)$$

It is well-known that SiO_2 is an acidic oxide.[133] Following Lewis' acid–base concepts, SiO_2 reacts with the basic oxide Na_2O to form a salt, sodium silicate. The thermodynamic activity of Na_2O (a_{Na_2O}) can be determined from the partial pressure of SO_3 and the free energy change ($\Delta G°$) of Eq. (45):

$$\Delta G°_{\text{Equation (45)}} = -2.303RT \log (P_{SO_3} a_{Na_2O}) \quad (47)$$

When Na_2SO_4 has a high activity of Na_2O, set by a low P_{SO_3}, it is called a basic molten salt. When Na_2SO_4 has a low activity of Na_2O, set by a high P_{SO_3}, it is called an acidic molten salt.

From purely thermodynamic considerations one can determine when Eq. (46) will occur. A threshold a_{Na_2O} for SiO_2 dissolution can be calculated from Eq. (46) as

$$\Delta G°_{\text{Equation (46)}} = 2.303RT \log a_{Na_2O} \quad (48)$$

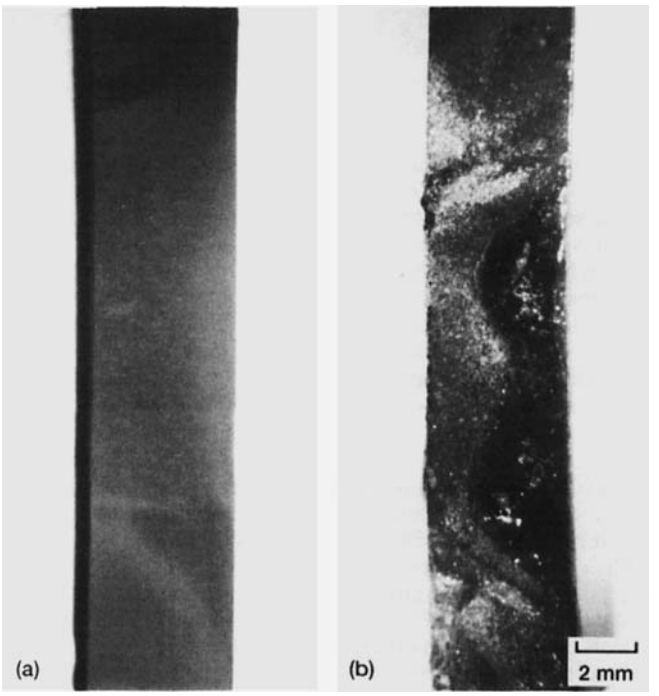

Fig. 25. Optical micrographs of sintered SiC with carbon and boron additives, treated in burner rig at 1273 K (leading edge is on the left): (a) 46 h with no sodium and (b) 13.5 h with 4-ppm sodium.

This border-line a_{Na_2O} for SiO_2 dissolution can be related to a corresponding P_{SO_3} by Eq. (47). Thus, one can calculate, for a given temperature, the threshold P_{SO_3} for dissolution. This is shown in Fig. 27. Note the temperature boundaries are the melting point of Na_2SO_4 and the dewpoint for Na_2SO_4 deposition. The values of P_{SO_3} from combustion of two typical fuels are also shown, as calculated by a free-energy-minimization program.[17,18] The intersection of this line with the shaded region in Fig. 27 shows when scale dissolution is expected. Experiments with quartz coupons in a burner rig verified these predictions, as shown in Fig. 28. The coupons treated in the low-sulfur fuel showed more corrosion, and chemical analysis revealed the presence of sodium silicate. The coupons treated in the high-sulfur fuel showed less corrosion, and chemical analysis revealed no sodium silicate.[18]

These calculations illustrate the value of the acid–base interpretation and provide general guidelines for predicting corrosion. However, as is often the case, the actual situation is more complex. Secondary elements can drive the molten salt more basic. It has been shown that SiC with excess carbon corrodes quite extensively in a situation where the P_{SO_3} is high enough to limit corrosion. The reason is that carbon tends to drive Na_2SO_4 basic.[18] An electrochemical cell can be used to measure a_{Na_2O} in a melt:[18,134]

$$Pt,O_2(r)|ZrO_2|Na_2SO_4,SO_3|\text{mullite}|10\text{-mol\%-}Ag_2SO_4,\ Na_2SO_4,Ag \quad (49)$$

Zirconia acts as a membrane for oxide anions, and the mullite acts as a membrane for sodium cations. They combine, and the net reaction is

$$Na_2O + Ag_2SO_4 = 0.5O_2 + Na_2SO_4 + 2Ag \quad (50)$$

At 1173 K, a_{Na_2O} is related to voltage (E) by

$$E = 1.498 + 0.116 \log a_{Na_2O} \quad (51)$$

Figure 29 shows the a_{Na_2O} measurements for $Na_2SO_4/(0.01SO_3 + O_2)$ and $Na_2SO_4/(0.01SO_3 + O_2)$ with added carbon. Note that the latter swings strongly basic. The most likely interpretation of this is the following sequence of reactions:

$$Na_2SO_4(l) + 2C = Na_2S + 2CO_2 \quad (52)$$

$$Na_2S + 3Na_2SO_4 = 4Na_2O + 4SO_2 \quad (53)$$

It is significant that carbon tends to drive Na_2SO_4 more basic because many types of SiC have excess carbon. These are more susceptible to hot corrosion.[130]

The reactive species Na_2O can form from other salts as well. Under some conditions Na_2CO_3 can deposit and decompose to

$$Na_2CO_3 = Na_2O + CO_2(g) \quad (54)$$

Na_2CO_3 tends to decompose more than Na_2SO_4, so that it is a more basic molten salt. McNallan *et al.*[135] have shown that Na_2O can also form from the reaction of sodium chloride (NaCl) and water vapor:

$$2NaCl + H_2O = Na_2O(s) + 2HCl \quad (55)$$

In both these reactions, if a_{Na_2O} is sufficiently high, SiO_2 is expected to dissolve.

Deposit-induced corrosion can also originate from vanadium compounds.[131,136–138] Vanadium pentoxide (V_2O_5) is an acidic oxide and therefore not expected to react with SiO_2. However, the phase diagram shows a limited solubility of SiO_2 in V_2O_5, which leads to accelerated rates.[136,138] Mixtures of Na_2SO_4 and V_2O_5 have led to severe corrosion of Si_3N_4.[137]

The concept of dissolution by basic molten salts can be extended to oxide slags as well. In the case of an oxide slag, it is more difficult to define and measure basicity. Generally, basicity is approximated by the ratio of basic to acidic oxides.[139] Ferber *et al.*[6] have identified three corrosion mechanisms from oxide slags. These are passivation by SiO_2, dissolution of SiO_2,

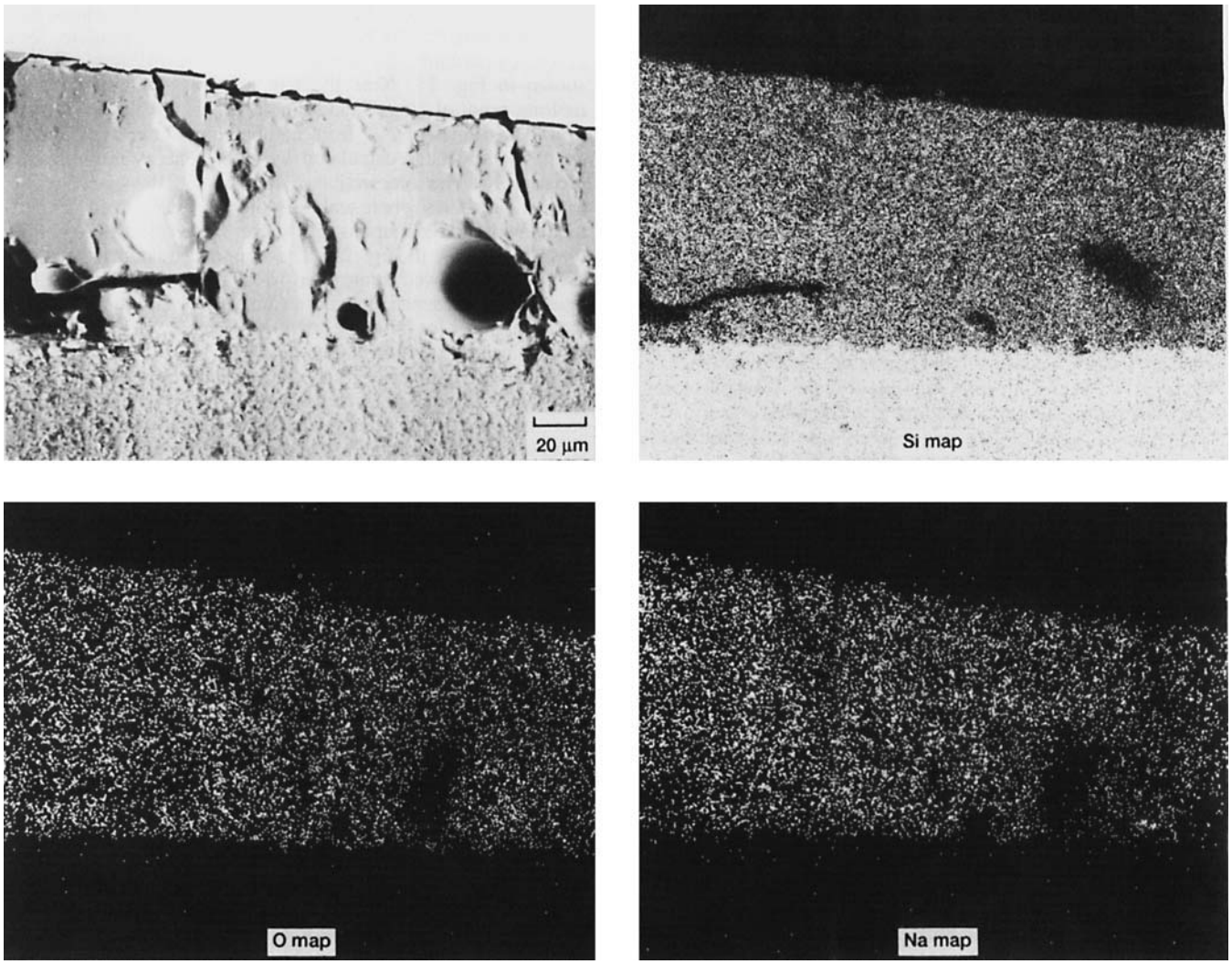

Fig. 26. Image and elemental maps of polished cross section of glassy products formed by burner rig corrosion at 1273 K with Jet A fuel for 13.5 h with 4-ppm sodium.

and formation of metal silicides at low oxygen potentials. Passivation is analogous to the reaction in Eq. (44) not proceeding; dissolution is analogous to the reaction in Eq. (44) proceeding.

(3) Kinetics of Deposit-Induced Corrosion

The kinetics of corrosion in Na_2SO_4 are consistent with this interpretation of dissolution and enhanced oxidation.[130] Kinetics of hot corrosion are studied in the laboratory by coating the specimen with Na_2SO_4 and following the kinetics on heating. This can be accomplished with a thermogravimetric analysis (TGA) system, such as that illustrated in Fig. 6. A one-time deposition of salt is not as realistic as continuous deposition in the burner; however, it does provide mechanistic information on the first stages of reaction.

Three situations can occur. The first is a basic molten salt, such as Na_2CO_3 or Na_2SO_4 in contact with carbon. This situation leads to the type of kinetic curve illustrated in Fig. 30. The early stages are characterized by a period of weight loss, which corresponds to the dissolution reaction. In this case the amount of weight loss corresponds very closely to that predicted from the reaction[130]

$$Na_2CO_3 + SiO_2 = Na_2SiO_3 + CO_2 \quad (56)$$

This is followed by a period of enhanced oxidation due to liquid scale. Finally, a protective SiO_2 layer forms below the melt, and the reaction slows. This final layered microstructure is shown in Fig. 31. This is consistent with the study of Mayer and Riley,[140] who saw rapid reaction until the Na_2O–SiO_2 liquidus was reached, at which point a stable tridymite film formed below the melt.

The second case is illustrated in Fig. 32. It has been shown that Na_2SO_4 with an overpressure of oxygen is sufficiently acidic so that SiO_2 is not expected to dissolve. Figure 32 shows a kinetic curve for Na_2SO_4/O_2 on Si_3N_4. The long period of weight loss corresponds to vaporization of Na_2SO_4; the rates are the same as those for Na_2SO_4 vaporizing from a platinum coupon. However, the period of weight gain corresponds to enhanced oxidation. Blachere and Pettit[95] have shown that even an acidic deposit can enhance oxidation by inducing devitrification and scale cracking or by doping the SiO_2 scale.

The third case leads to the most extreme corrosion.[130] This is illustrated by the data in Table VIII. In this case $Na_2SO_4/(0.01SO_3 + O_2)$, a very acidic salt, is used. Chemical analysis of the scale indicates limited attack in the presence of this salt on the SiC and Si_3N_4 with oxide additives. However, for the SiC with carbon additives, extensive attack occurs. This is explained by the basic effect of carbon at the bottom of the melt and the acidic effect of Na_2SO_4/SO_3 at the top of the melt. These effects create the reaction sequence illustrated in Fig. 33. This self-sustaining series of reactions can lead to severe corrosion. It is termed "fluxing" and is well-known from the hot corrosion of metals.[128,129]

In summary, hot corrosion occurs only in a limited regime. However, it can be quite severe, and, therefore, it is important

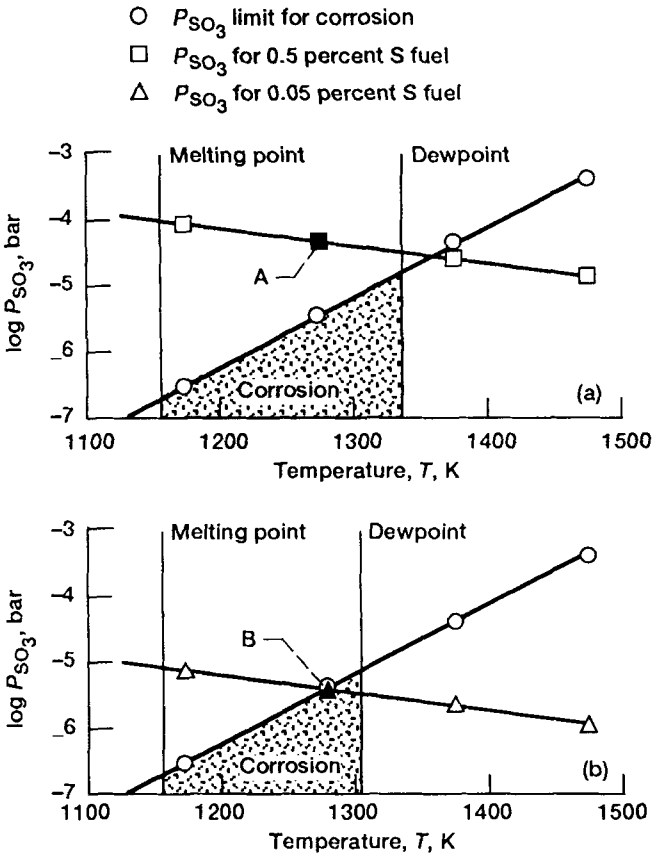

Fig. 27. Calculated corrosion regimes for SiO_2: (a) 0.5% sulfur fuel, 2-ppm sodium, 0.025 fuel-to-air ratio, 1273 K, and (b) 0.05% sulfur fuel, 2-ppm sodium, 0.025 fuel-to-air ratio, 1273 K.

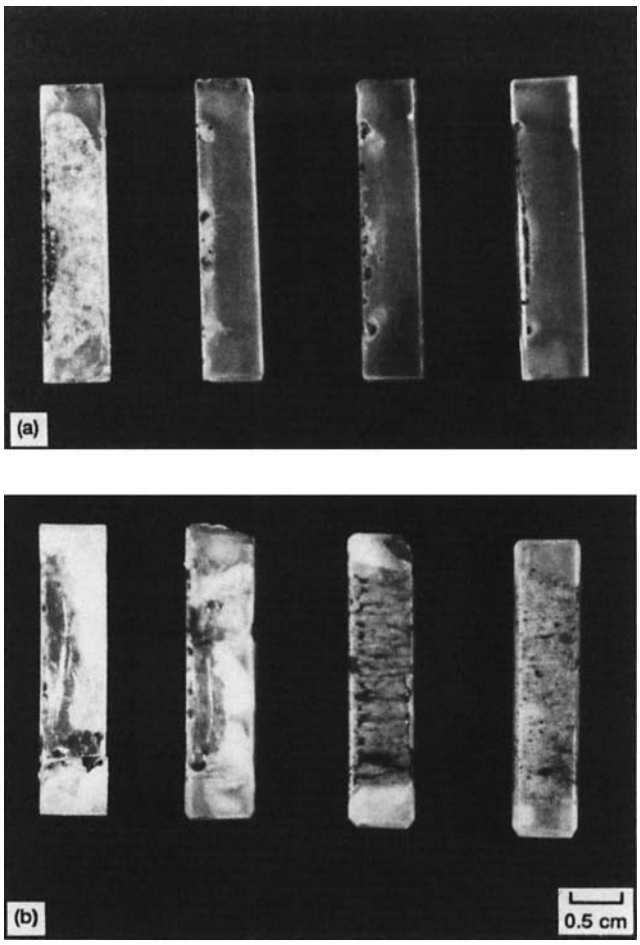

Fig. 28. SiO_2 coupons treated in burner rig in 2-ppm sodium at 1273 K: (a) No. 2 diesel fuel (0.5% sulfur), 5 h (point A on Fig. 27(a)), and (b) Jet A fuel (0.05% sulfur), 1 h (point B on Fig. 27(b)).

to be cognizant of when it occurs. The dissolution reactions in hot corrosion allow corrosion regimes to be predicted. These reactions are best interpreted in terms of the acid–base theory of oxide reactions.

XII. Composites

This review has concentrated on the near-surface durability of the SiO_2-protected SiC and Si_3N_4 systems. Thus, the conclusions apply to monolithic SiC and Si_3N_4 and composites of these materials. Currently there is much interest in SiC-fiber-reinforced SiC and Si_3N_4 matrices. These composites may have some unique oxidation and corrosion properties, and it is important to mention them.

At their current state of development, these materials may be porous and contain secondary elements, such as refractory oxides and/or carbon. These effects have been discussed. In addition, composites require fiber coatings to prevent bonding of the fibers to the matrix. Loosely bonded fibers permit effective crack bridging and crack deflection, which lead to a tougher ceramic.[141] However, the current fiber coatings, carbon or boron nitride (BN), are quite susceptible to oxidation if a path for oxygen is available. Thus, oxidation may lead to a degradation of the critical fiber interface and loss in properties. Some composites have exhibited a low-temperature oxidation problem due to inadequate coverage of the passivating SiO_2 scale, which then allows oxygen penetration to the fiber coatings.[142] Recent work by Filipuzzi and Naslain[143,144] critically examines oxidation of composites from both an experimental and theoretical point of view. Their study presents important results on the effect of temperature and carbon coating thickness on SiC fibers. Lower temperatures lead to slower oxidation rates of the carbon coating, but along a long length of the fiber; higher temperatures lead to more rapid oxidation, but along a short length of the fiber. They also show that a thinner fiber coating is desirable, since it leads to healing more readily than thicker coatings. Improvement in oxidation and corrosion properties is an important driving force in composite development.

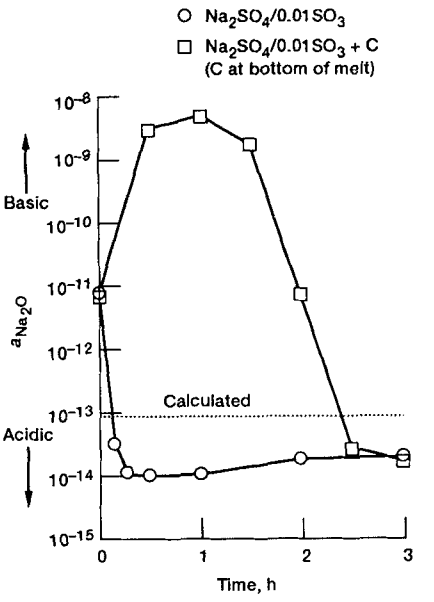

Fig. 29. Effect of carbon on basicity of Na_2SO_4.

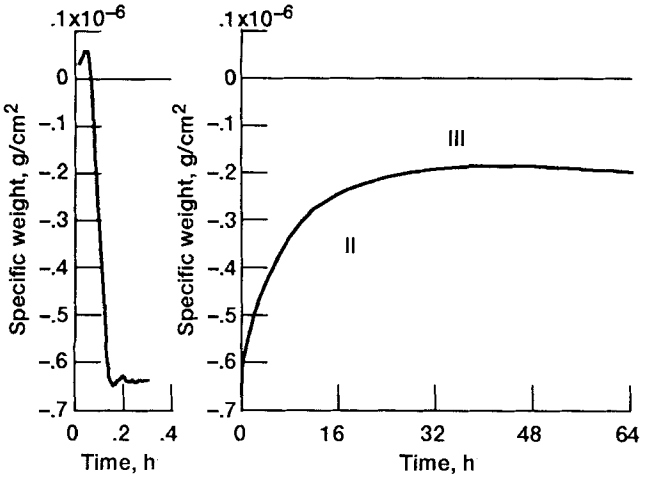

Fig. 30. Kinetics for SiC + Na_2CO_3.

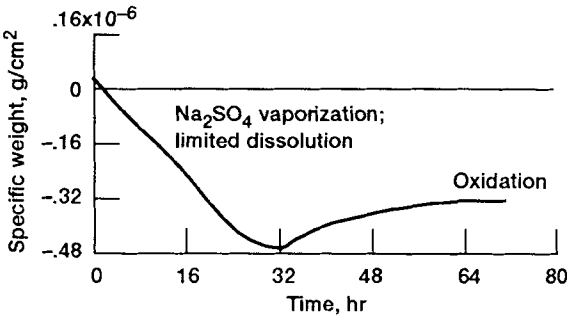

Fig. 32. Kinetics for Si_3N_4 + Na_2SO_4.

XIII. Corrosion and Degradation of Mechanical Properties

The focus of this paper has been on chemical mechanisms of degradation. A major issue has been the assessment of this degradation. An assessment in terms of microstructural changes

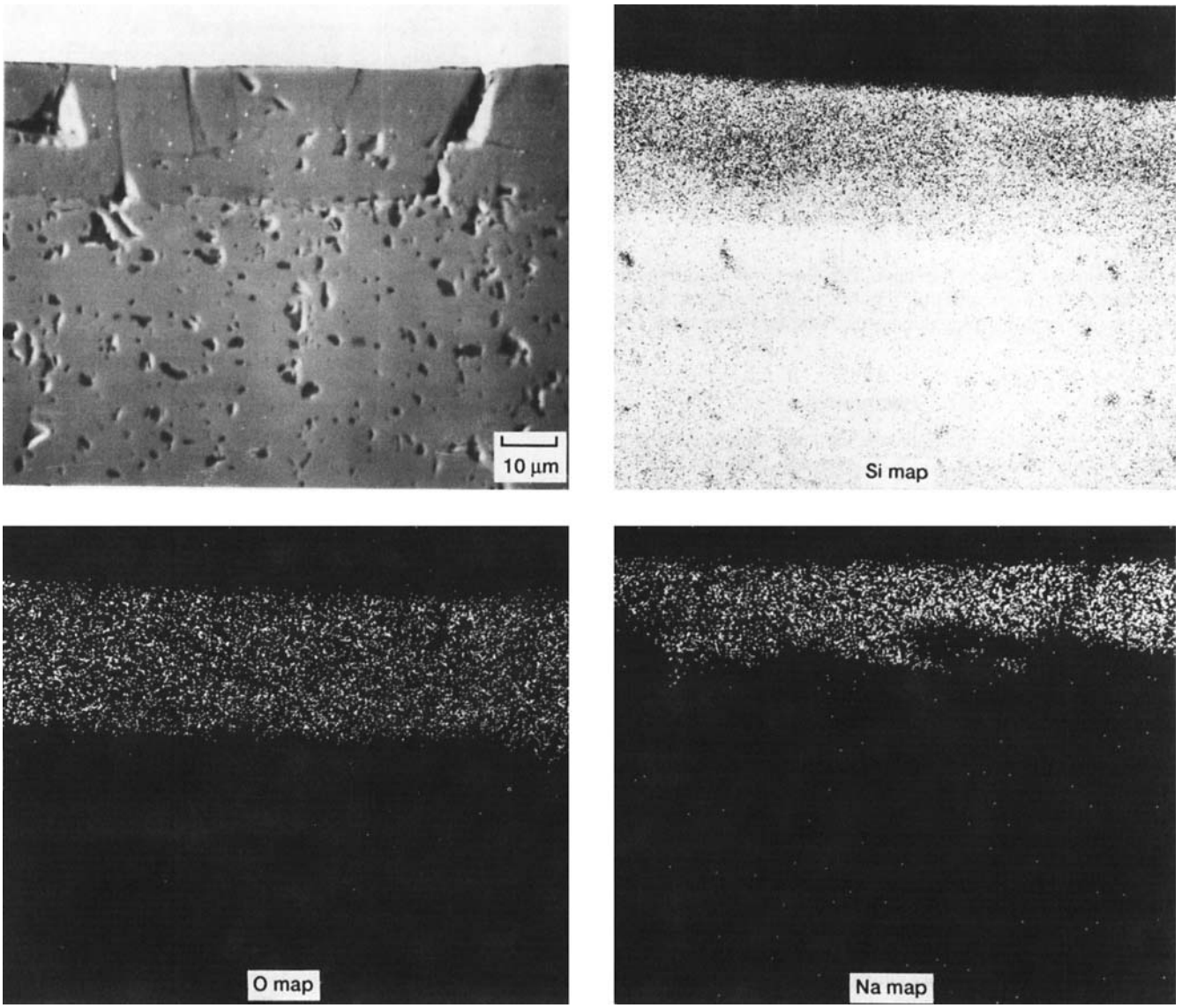

Fig. 31. Polished cross section showing final microstructure for SiC + Na_2CO_3 after 48 h of reaction.

Table VIII. Quantity of Corrosion Products[130,1]

Material	Na_2SO_4 (mg/cm²)	$Na_2O{\cdot}x(SiO_2)$ (mg/cm²)	x	SiO_2 (mg/cm²)
Single-crystal SiC	1.64 ± 0.86	<0.01		1.82 ± 0.96
Hot-pressed SiC with Al_2O_3	2.01 ± 0.03	<.01		0.39 ± 0.02
Sintered SiC with B and C	0.49 ± 0.06	0.97 ± 0.28	1.6 ± 0.9	10.50 ± 0.66
Sintered Si_3N_4 with Y_2O_3 and Al_2O_3	0.23 ± 0.11			1.3 ± 0.2

[1] $Na_2SO_4/(0.01SO_3 + O_2)$; 48 h, 1273 K.

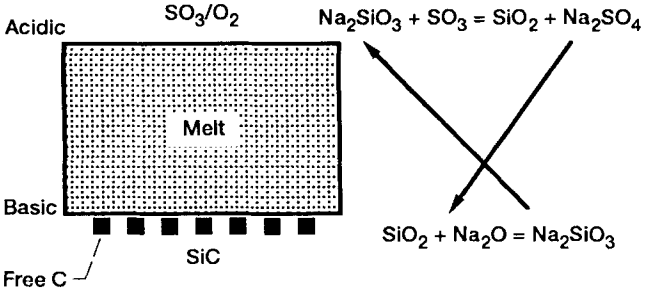

Fig. 33. Schematic of fluxing mechanism operative in carbon-saturated SiC + Na_2SO_4 case.

may be sufficient in a fundamental study, but the designer needs to know how these changes affect properties such as strength, fracture toughness, fatigue, and creep. A thorough discussion of this is beyond the scope of this paper. However, a few comments are appropriate.

Many of the studies in this area deal with the change in mechanical properties after corrosion.[145-151] However, applied stress and corrosion often act synergistically. For example, the oxidation rate of reaction-sintered Si_3N_4/SiC material increases with applied stress.[149] In a recent review, Tressler[152] has discussed corrosion-induced effects on critical flaw generation, crack growth, and creep behavior.

It has been shown that limited oxidation tends to blunt cracks and may actually increase strength.[76,145,146] However, long-term oxidation[147] and molten salt corrosion[148,150,151] lead to extensive pitting, as shown in Fig. 34. In a monolithic ceramic, pitting leads to substantial strength reductions. As more flaw-resistant ceramics and composites are developed, the issue of surface flaws should become less important.

Corrosion also changes mechanical properties by influencing crack growth.[152] This is particularly critical in the case of materials with a second phase at the grain boundary. High-temperature oxidation may lead to crystallization and compositional changes in this phase, which may lower the threshold stress intensity for crack growth.[152] The corrosion reactions at or near the crack tip are quite critical,[153,154] analogous with moisture-assisted crack growth in ceramics.[155] Henager and Jones[154] have shown that the presence of molten Na_2SO_4 on Si_3N_4 increases the velocity of slow crack growth by a factor of 2 over air at 1573 K. Relatively little is known about the effects of corrosion on creep in SiC. In Si_3N_4, grain-boundary phase and/or compositional changes due to oxidation are expected to alter the creep rate.[152]

The discussion thus far has centered on monolithic ceramics. In the case of fiber-reinforced composites, other issues, such as oxidation-induced fiber/matrix bonding, must be considered.[156] The issue here is how much fiber/matrix bonding can be tolerated before an unacceptable loss in composite properties occurs.

In summary, the synergistic linkage of mechanical properties and corrosion is an important area of research toward applying silicon-based ceramics as structural components. Only a few key issues have been discussed here; the reader is referred to other reviews for a more thorough discussion.[152,153]

XIV. Summary and Conclusions

Many proposed applications of silicon-based ceramics involve exposure to combustion gases. These environments have been defined and shown to vary depending on the application. All involve high temperatures and most are highly oxidizing. Some have components that may lead to condensed-phase deposits.

Five types of corrosive degradation have been identified: passive oxidation, deposit-induced corrosion, active oxidation, scale/substrate interactions, and scale volatilization. A fundamental understanding of the oxidation process is emerging from studies on pure materials in pure oxygen. The key issues are transport through the SiO_2 scale, rate-controlling steps, and the differences between SiC and Si_3N_4. Commercial materials in combustion environments add a number of complexities to the fundamental oxidation process. These include crystallization of the SiO_2 film, additive effects, H_2O and CO_2 as oxidants, thermal cycling effects, and combustion gas impurity effects. In

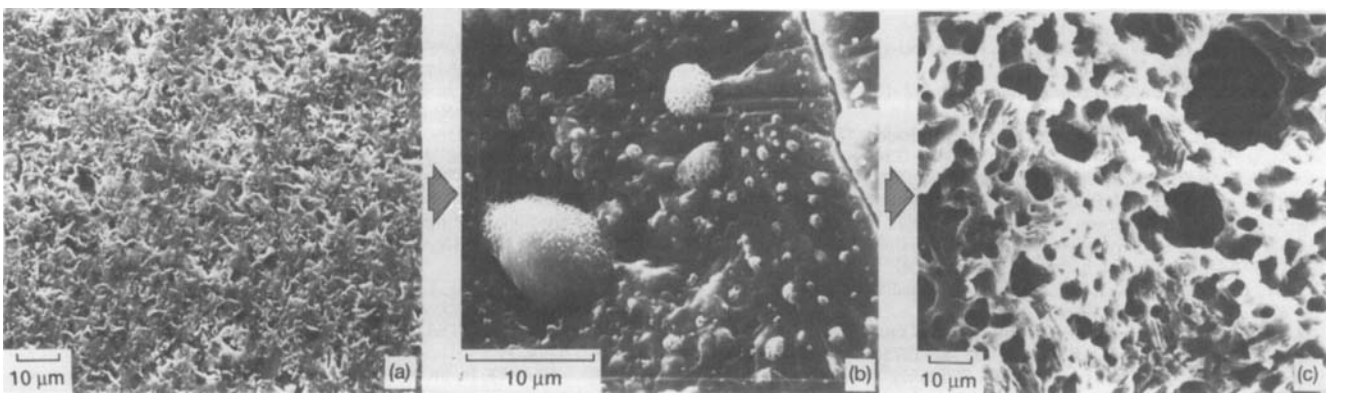

Fig. 34. Sequence showing sintered SiC with boron and carbon additives before corrosion, after corrosion with $Na_2SO_4/(0.01SO_3 + O_2)$ at 1273 K for 48 h, showing glassy product layer, and with glassy product layer removed by HF etch, revealing extensive pitting of SiC.

addition, some low-oxidant atmospheres can lead to active oxidation.

The use of silicon-based ceramics is limited at very high temperatures because of rapid oxidation, volatility, scale-melting, and scale/substrate reactions. Volatility is an issue in some atmospheres. Scale melting is a limitation at 1996 K. Finally, scale/substrate reactions may lead to extensive bubbling and are an issue for carbon-rich SiC.

Condensed-phase deposits are an issue in a narrow region at lower temperatures but can be quite severe. These reactions can be understood from the acid–base theory of oxides.

In general, our understanding of the response of SiO_2 scales to combustion environments lags behind that of Al_2O_3 and Cr_2O_3 on metallic alloys. Many important aspects remain to be explored both in the chemistry of these interactions and in the correlation of corrosion with mechanical properties.

Acknowledgments: It is a pleasure to acknowledge the many helpful discussions I had in preparing this paper. In the combustion area, I would like to thank D. Blint of GM Research Laboratories and G. Seng of NASA Lewis. In the oxidation area, I would like to thank J. Smialek, L. Ogbuji, D. Fox, and E. Opila of NASA Lewis; K. Luthra of General Electric CR&D, Schenectady, NY; R. Tressler of The Pennsylvania State University, University Park, PA; and J. Porter II of MSNW, Inc., San Marcos, CA.

References

[1]G. L. Boyd and D. M. Kreiner, "AGT101/Advanced Turbine Technology Applications Project (ATTAP)"; pp. 275–80 in *Proceedings of the Twenty-Sixth Automotive Technology Development Contractors' Coordination Meeting*, P-219. Society of Automotive Engineers, Warrendale, PA, 1989.

[2]G. H. Callum and T. E. Schmid, "Ceramic Composites for Aircraft Gas Turbine Engines," AIAA Paper No. 91-1892. American Institute of Aeronautics and Astronautics, Washington, DC, June 1991.

[3]A. Bennett, "Requirements for Engineering Ceramics in Gas Turbine Engines," *Mater. Sci. Technol.*, **2**, 895–99 (1986).

[4]A. F. McLean, "Materials Approach to Engine/Component Design"; pp. 1023–34 in *Ceramic Materials and Components for Engines*, Proceedings of the Second International Symposium. Edited by W. Bunk and H. Hausner. Verlag Deutsche Keramische Gesellschaft, Bad Honnef, Germany, 1986.

[5]J. I. Federer, T. N. Tiegs, D. M. Kotchick, and D. Petrak, "Analysis of Candidate Silicon Carbide Recuperator Materials Exposed to Industrial Furnace Environments," Rept. No. ORNL/TM-9677, Oak Ridge National Laboratory, Oak Ridge, TN, July 1985.

[6]M. K. Ferber, J. Ogle, V. J. Tennery, and T. Henson, "Characterization of Corrosion Mechanisms Occurring in a Sintered SiC Exposed to Basic Coal Slags," *J. Am. Ceram. Soc.*, **68** [4] 191–97 (1985).

[7]D. P. Butt, R. E. Tressler, and K. E. Spear, "Durability of SiC Materials in Gaseous N_2–H_2–CO Heat Treat Environments: I," *Ind. Heat.*, **58** [9] 44–48 (1991).

[8]N. J. Shaw *et al.*, "Materials for Engine Applications Above 3000°F—An Overview," NASA Rept. No. TM-100169, NASA Lewis Research Center, Cleveland, OH, 1987.

[9]H. Du, R. E. Tressler, and C. G. Pantano, "Oxidation Studies of Crystalline CVD Silicon Nitride," *J. Electrochem. Soc.*, **136** [5] 1527–36 (1989).

[10]R. Pampuch, W. Ptak, S. Jonas, and J. Stoch, "Formation of Ternary Si-O-C Phase(s) During Oxidation of SiC," *Mater. Sci. Monogr.*, **6**, 435–48 (1980).

[11]J. L. Smialek and G. H. Meier, "High-Temperature Oxidation"; pp. 293–326 in *Superalloys II*. Edited by C. T. Sims, N. S. Stoloff, and W. C. Hagel. Wiley, New York, 1988.

[12]J. H. Gary and G. E. Hardwick, *Petroleum Refining: Technology and Economics*; p. 32. Marcel Dekker, New York, 1975.

[13]North American Combustion Handbook, 2nd ed.; p. 16. North American Manufacturing Co., Cleveland, OH, 1978.

[14]"Standard Specifications for Automotive Gasoline," ASTM Designation D 439-89. *1991 Book of ASTM Standards*. American Society for Testing and Materials, Philadelphia, PA.

[15]V. Valkovic, *Trace Elements in Petroleum*; pp. 62–101. PPE Books, Tulsa, OK, 1978.

[16]R. H. Jungers, R. E. Lee, Jr., and D. J. von Lehmden, "The EPA National Fuels Surveillance Network. I. Trace Constituents in Gasoline and Commercial Gasoline Fuel Additives," *Environ. Health Perspect.*, **10**, 143–50 (1975).

[17]S. Gordon and B. J. McBride, "Computer Program for the Calculation of Complex Chemical Equilibrium Compositions, Rocket Performance, Incident and Reflected Shocks, and Chapman–Jouget Detonations," NASA Rept. No. SP-273, NASA Lewis Research Center, Cleveland, OH, 1971.

[18]N. S. Jacobson, "Sodium Sulfate: Deposition and Dissolution of Silica," *Oxid. Met.*, **31** [1/2] 91–103 (1989).

[19]J. B. Heywood, "Pollutant Formation and Control in Spark-Ignition Engines," *Prog. Energy Combust. Sci.*, **1**, 135–64 (1975).

[20]M. K. Hossain, A. C. Noke, and S. R. J. Saunders, "Oxidation of a Ni–Cr–Al Alloy at 850°C in Air Containing HCl Gas," *Oxid. Met.*, **12** [5] 451–71 (1978).

[21]W. D. Kingery, H. K. Bowen, and D. R. Uhlmann, *Introduction to Ceramics*, 2nd ed.; p. 595. Wiley, New York, 1976.

[22]M. P. Murrell, C. J. Sofield, and S. Sugden, "Silicon Transport During Oxidation," *Philos. Mag. B*, **63** [6] 1277–87 (1991).

[23]J. A. Costello and R. E. Tressler, "Oxidation Kinetics of Hot-Pressed and Sintered α-SiC," *J. Am. Ceram. Soc.*, **64** [6] 327–31 (1981).

[24]R. L. Meek, "Diffusion Coefficient for Oxygen in Vitreous SiO_2," *J. Am. Ceram. Soc.*, **56** [6] 341–42 (1973).

[25]A. G. Revesz and H. A. Schaeffer, "The Mechanism of Oxygen Diffusion in Vitreous SiO_2," *J. Electrochem. Soc.*, **129** [2] 357–61 (1982).

[26]F. J. Norton, "Gas Permeation Through the Vacuum Envelope"; pp. 8–16 in *Transactions of the Eighth National Vacuum Symposium*. Edited by L. E. Preuss. Pergamon Press, New York, 1962.

[27]E. W. Sucov, "Diffusion of Oxygen in Vitreous Silica," *J. Am. Ceram. Soc.*, **46** [1] 14–20 (1963).

[28]E. L. Williams, "Diffusion of Oxygen in Fused Silica," *J. Am. Ceram. Soc.*, **48** [4] 190–94 (1965).

[29]K. Muehlenbachs and H. A. Schaeffer, "Oxygen Diffusion in Vitreous Silica—Utilization of Natural Isotopic Abundances," *Can. Mineral.*, **15**, 179–84 (1977).

[30]J. D. Cawley, "Oxygen Tracer Diffusion in Vitreous Silica"; presented at the 94th Annual Meeting of the American Ceramic Society, Minneapolis, MN, April 14, 1992 (A. R. Cooper Symposium, Paper No. 2-JX111-92), *J. Am. Ceram. Soc.*, in review.

[31]B. E. Deal and A. S. Grove, "General Relationship for the Thermal Oxidation of Silicon," *J. Appl. Phys.*, **36** [12] 3770–78 (1965).

[32]R. H. Doremus, "Oxidation of Silicon: Tests of Mechanisms"; pp. 17–23 in *The Physics and Chemistry of SiO_2 and the Si–SiO_2 Interface*. Edited by C. R. Helms and B. E. Deal. Plenum Press, New York, 1988.

[33]J. A. Costello and R. E. Tressler, "Isotope Labeling Studies of the Oxidation of Silicon at 1000°C and 1300°C," *J. Electrochem. Soc.*, **131** [8] 1944–47 (1984).

[34]J. D. Cawley, J. W. Halloran, and A. R. Cooper, "Oxygen-18 Tracer Study of the Passive Thermal Oxidation of Silicon," *Oxid. Met.*, **28** [1/2] 1–16 (1987).

[35]E. Fitzer and R. Ebi, "Kinetic Studies on the Oxidation of Silicon Carbide"; pp. 320–28 in *Silicon Carbide 1973*. Edited by R. C. Marshall, J. W. Faust, Jr., and C. E. Ryan. University of South Carolina Press, Columbia, SC, 1974.

[36]S. Lin, "Mass Spectrometric Analysis of the Vapors in Oxidation of Si_3N_4 Compacts," *J. Am. Ceram. Soc.*, **58** [3–4] 160 (1975).

[37]M. Wakamatsu, N. Takeuchi, and T. Hattori, "Oxidation of Sintered Si_3N_4 at 1400°C in Oxygen Atmosphere"; pp. 1694–703 in *UNITECR '89*, Proceedings of the United International Technical Conference on Refractories. Edited by L. J. Trostel, Jr. American Ceramic Society, Westerville, OH, 1989.

[38]K. L. Luthra, "Some New Perspectives on Oxidation of Silicon Carbide and Silicon Nitride," *J. Am. Ceram. Soc.*, **74** [5] 1095–103 (1991).

[39]J. Schlicting, "Siliciumcarbid Als Oxidationbestandiger Hochtemperaturwerkstoff; Oxidations-und Heisddkorrosions-Verhalten I," *Ber. Dtsch. Keram. Ges.*, **56** [8] 196–200 (1979).

[40]J. W. Fergus and W. L. Worrell, "Oxidation of Chemically Vapor Deposited Silicon Carbide"; pp. 43–52 in Ceramic Transactions, Vol. 10, *Corrosion and Corrosive Degradation of Ceramics*. Edited by R. E. Tressler and M. McNallan. American Ceramic Society, Westerville, OH, 1990.

[41]G. H. Schiroky, R. J. Price, and J. E. Sheehan, "Oxidation Characteristics of CVD Silicon Carbide and Silicon Nitride," Rept. No. GA-A18696, GA Technologies, Inc., San Diego, CA, 1986.

[42]J. A. Costello and R. E. Tressler, "Oxidation of Silicon Carbide Crystals and Ceramics: I, In Dry Oxygen," *J. Am. Ceram. Soc.*, **69** [9] 674–81 (1986).

[43]C. D. Fung and J. J. Kopanski, "Thermal Oxidation of 3C Silicon Carbide Single-Crystal Layers on Silicon," *Appl. Phys. Lett.*, **45** [7] 757–59 (1984).

[44]L. Muehlhoff, M. J. Bozack, W. J. Choyke, and J. T. Yates, Jr., "Comparative Oxidation Studies of SiC(000$\bar{1}$) and SiC(0001) Surfaces," *J. Appl. Phys.*, **60** [7] 2558–63 (1986).

[45]E. J. Opila, "The Oxidation Kinetics of Chemically Vapor Deposited Silicon Carbide"; presented at TMS Fall Meeting, Chicago, IL, 1992.

[46]K. Motzfeld, "On the Rates of Oxidation of Silicon and Silicon Carbide in Oxygen and Correlation with Permeability of Silica Glass," *Acta Chem. Scand.*, **18** [7] 1596–606 (1964).

[47]Z. Zheng, R. E. Tressler, and K. E. Spear, "Oxidation of Single-Crystal Silicon Carbide, Part I. Experimental Studies," *J. Electrochem. Soc.*, **137** [3] 854–58 (1990).

[48]Z. Zheng, R. E. Tressler, and K. E. Spear, "Oxidation of Single-Crystal Silicon Carbide, Part II. Kinetic Model," *J. Electrochem. Soc.*, **137** [9] 2812–16 (1990).

[49]J. D. Cawley and R. S. Boyce, "A Solution of the Diffusion Equation for Double Oxidation in Dry Oxygen Including Lazy Exchange Between Network and Interstitial Oxygen," *Philos. Mag. A*, **58** [4] 589–601 (1988).

[50]P. Kofstad, *High-Temperature Oxidation of Metals*; p. 125. Wiley, New York, 1966.

[51]T. Narushima, T. Goto, and T. Hirai, "High-Temperature Passive Oxidation of Chemically Vapor Deposited Silicon Carbide," *J. Am. Ceram. Soc.*, **72** [8] 1386–90 (1989).

[52]D. M. Mieskowski, T. E. Mitchell, and A. H. Heuer, "Bubble Formation in Oxide Scales on SiC," *J. Am. Ceram. Soc.*, **67** [1] C-17–C-18 (1984).

[53]R. C. A. Harris, "Oxidation of 6-H SiC Platelets," *J. Am. Ceram. Soc.*, **58** [1–2] 7–9 (1975).

[54]D. J. Choi, D. B. Fischbach, and W. D. Scott, "Oxidation of Chemically-Vapor-Deposited Silicon Nitride and Single-Crystal Silicon," *J. Am. Ceram. Soc.*, **72** [7] 1118–23 (1989).

[55]T. Hirai, K. Nihara, and T. Goto, "Oxidation of CVD Si_3N_4 at 1550°C to 1650°C," *J. Am. Ceram. Soc.*, **63** [7–8] 419–24 (1980).

[56]H. Du, C. A. Houser, R. E. Tressler, K. E. Spear, and C. G. Pantano, "Isotropic Studies of Oxidation of Si_3N_4 and Si Using SIMS," *J. Electrochem. Soc.*, **137** [2] 741–42 (1990).

[57]H. Du, R. E. Tressler, and K. E. Spear, "Thermodynamics of the Si-N-O System and Kinetic Modeling of Oxidation of Si_3N_4," *J. Electrochem. Soc.*, **136** [11] 3210–15 (1989).

[58]K. L. Luthra, "A Mixed Interface Reaction/Diffusion Control Model for Oxidation of Si_3N_4," *J. Electrochem. Soc.*, **138** [10] 3001–3007 (1991).

[59]L.U.J.T. Ogbuji, "Role of Si_2N_2O in the Passive Oxidation of Chemically-Vapor-Deposited Si_3N_4," *J. Am. Ceram. Soc.*, **75** [11] 2995–3000 (1992).

[60]A. H. Heuer, L. U. Ogbuji, and T. E. Mitchell, "The Microstructure of Oxide Scales on Oxidized Si and SiC Single Crystals," *J. Am. Ceram. Soc.*, **63** [5–6] 354–55 (1980).

[61]S. C. Singhal, "Oxidation Kinetics of Hot-Pressed Silicon Carbide," *J. Mater. Sci.*, **11**, 1246–53 (1976).

[62]S. C. Singhal and F. F. Lange, "Effect of Alumina Content on the Oxidation of Hot-Pressed Silicon Carbide," *J. Am. Ceram. Soc.*, **58** [9–10] 433–35 (1975).

[63]S. C. Singhal, "Oxidation and Corrosion–Erosion Behavior of Si_3N_4 and SiC"; pp. 533–48 in *Ceramics for High-Performance Applications*. Edited by J. J. Burke, A. E. Gorum, and R. N. Katz. Metals and Ceramics Information Center, Columbus, OH, 1974.

[64]S. C. Singhal, "Thermodynamics and Kinetics of Oxidation of Hot-Pressed Silicon Nitride," *J. Mater. Sci.*, **11**, 500 (1976).

[65]V. A. Lavrenko, I. G. Gogotsi, A. B. Goncharuk, A. F. Alekseev, O. N. Grigorev, and O. D. Shcherbina, "High-Temperature Oxidation of Reaction-Sintered Silicon Nitride with Various Additions," *Poroshk. Metall.*, **267** [3] 35–39 (1985).

[66]J. W. Hinze, W. C. Tripp, and H. C. Graham, "The High-Temperature Oxidation of Hot-Pressed Silicon Carbide"; pp. 405–19 in *Mass Transport Phenomena in Ceramics*. Edited by A. R. Cooper and A. H. Heuer. American Ceramic Society, Columbus, OH, 1975.

[67]J. A. Costello, R. E. Tressler, and I. S. T. Tsong, "Boron Redistribution in Sintered α-SiC During Thermal Oxidation," *J. Am. Ceram. Soc.*, **64** [6] 332–35 (1981).

[68]D. Cubicciotti and K. Lau, "Kinetics of Oxidation of Hot-Pressed Silicon Nitride Containing Magnesia," *J. Am. Ceram. Soc.*, **61** [11–12] 512–17 (1978).

[69]D. Cubicciotti and K. H. Lau, "Kinetics of Oxidation of Yttria Hot-Pressed Silicon Nitride," *J. Electrochem. Soc.*, **126** [10] 1723–28 (1979).

[70]W. C. Tripp and H. C. Graham, "Oxidation of Si_3N_4 in the Range 1300° to 1500°C," *J. Am. Ceram. Soc.*, **59** [9–10] 399–403 (1976).

[71]P. Andrews and F. L. Riley, "The Microstructure and Composition of Oxide Films Formed During High-Temperature Oxidation of a Sintered Si_3N_4," *J. Eur. Ceram. Soc.*, **5**, 245–56 (1989).

[72]J. Schlichting and L. J. Gauckler, "Oxidation of Some β-Si_3N_4 Materials," *Powder Metall. Int.*, **9** [1] 36–39 (1977).

[73]D. R. Clarke, "Thermodynamic Mechanism for Cation Diffusion Through an Intergranular Phase: Applications to Environmental Reactions with Nitrogen Ceramics"; pp. 421–26 in *Progress in Nitrogen Ceramics*, NATO ASI Series, Series E: Applied Sciences, No. 65. Edited by F. L. Riley. Martinus Nijhoff, The Hague, Netherlands, 1983.

[74]J. Chen, J. Sjoger, O. Lindqvist, C. O'Meara, and L. Pejryd, "The Rate-Controlling Processes in the Oxidation of HIPed Si_3N_4 with and without Sintering Additives," *J. Eur. Ceram. Soc.*, **7**, 319–27 (1991).

[75]J. K. Patel and D. P. Thompson, "The Low-Temperature Oxidation Problem in Yttria-Densified Silicon Nitride Ceramics," *Br. Ceram. Trans. J.*, **87**, 70–73 (1988).

[76]A. G. Evans and R. W. Davidge, "The Strength and Oxidation of Reaction-Sintered Silicon Nitride," *J. Mater. Sci.*, **5**, 314 (1970).

[77]F. Porz and F. Thummler, "Oxidation Mechanism of Porous Silicon Nitride," *J. Mater. Sci.*, **19**, 1283–95 (1984).

[78]J. E. Antill and J. B. Warburton, "Oxidation of Silicon and Silicon Carbide in Gaseous Atmospheres at 1000°–1300°C"; in *Reactions Between Solids and Gases*, AGARD CP-52. Advisory Group for Aerospace Research and Development, Paris, France, 1970.

[79]J. B. Warburton, J. E. Antill, and R. W. M. Hawes, "Oxidation of Thin-Sheet Reaction-Sintered Silicon Nitride," *J. Am. Ceram. Soc.*, **61**, 67–72 (1978).

[80]D. S. Fox, "Oxidation Kinetics of CVD Silicon Carbide and Silicon Nitride," *Ceram. Eng. Sci. Proc.*, **13** [9–10] 836–43 (1992).

[81]C. E. Lowell, J. L. Smialek, and C. A. Barrett, "Cyclic Oxidation of Superalloys"; pp. 219–26 in *High-Temperature Corrosion*, Proceedings of the International Conference. Edited by R. A. Rapp. NACE, Houston, TX, 1983.

[82]Y. S. Touloukian, R. K. Kirby, R. E. Taylor, and T. Y. R. Lee, *Thermal Expansion of Nonmetallic Solids*, Thermophysical Properties of Matter, Vol. 13; pp. 350, 358, 873, and 1140. IFI/Plenum, New York, 1970.

[83]E. J. Opila, D. S. Fox, and C. A. Barrett, "Cyclic Oxidation of Monolithic SiC and Si_3N_4 Materials"; to be presented at the 17th Annual Conference on Composites and Advanced Ceramics (Paper No. ECDCB 93-44), Cocoa Beach, FL, 1993.

[84]L. J. Lindberg, "Durability Testing of Ceramic Materials for Turbine Engine Applications"; pp. 149–61 in *Proceedings of the Twenty-Fourth Automotive Technology Development Contractors' Coordination Meeting*, P-197. Society of Automotive Engineers, Warrendale, PA, 1986.

[85]L. Lindberg, "Cyclic Oxidation of Advanced Silicon Nitrides"; pp. 79–86 in *Proceedings of the Annual Automotive Technology Development Contractors' Meeting*. Society of Automotive Engineers, Warrendale, PA, 1991.

[86]M. Maeda, K. Nakamura, T. Ohkubo, J. Ito, and E. Ishii, "Oxidation Behavior of Silicon Nitride under Static and Cyclic Conditions," *Ceram. Int.*, **15**, 247–53 (1989).

[87]P. Andrews and F. Riley, "Oxidation of Silicon Nitride during High-Temperature Thermal Cycling"; pp. 259–70 in *Advanced Engineering with Ceramics*. British Ceramic Society Proceedings, No. 46. The Institute of Ceramics, Shelton, U.K., 1990.

[88]A. J. Moulson and J. P. Roberts, "Water in Silica Glass," *Trans. Faraday Soc.*, **57**, 1208–16 (1961).

[89]E. A. Irene and R. Ghez, "Silicon Oxidation Studies: The Role of H_2O," *J. Electrochem. Soc.*, **124** [11] 1757–61 (1977).

[90]P. J. Jorgensen, M. E. Wadsworth, and I. B. Cutler, "Effects of Water Vapor on Oxidation of Silicon Carbide," *J. Am. Ceram. Soc.*, **44** [6] 258–61 (1961).

[91]H. Cappelen, K. H. Johansen, and K. Motzfeld, "Oxidation of Silicon Carbide in Oxygen and Water Vapor at 1500°C," *Acta Chem. Scand. A*, **35**, 247–54 (1981).

[92]T. Narushima, T. Goto, Y. Iguchi, and T. Hirai, "High-Temperature Oxidation of Chemically Vapor-Deposited Silicon Carbide in Wet Oxygen at 1823 to 1923 K," *J. Am. Ceram. Soc.*, **73** [12] 1580–84 (1990).

[93]M. Maeda, K. Nakamura, and T. Ohkubo, "Oxidation of Silicon Carbide in a Wet Atmosphere," *J. Mater. Sci.*, **23**, 3933–38 (1988).

[94]R. E. Tressler, J. A. Costello, and Z. Zheng, "Oxidation of Silicon Carbide Ceramics"; pp. 307–14 in *Industrial Heat Exchangers*. Edited by A. J. Hayes, *et al.* American Society of Metals, Warrendale, PA, 1985.

[95]J. R. Blachere and F. S. Pettit, "High-Temperature Corrosion of Ceramics," Rept. No. DOE/ER-45117-1 for the U.S. Department of Energy under Contract No. DE-FG02-84ER-45117 by the Department of Metallurgical and Materials Engineering, University of Pittsburgh, Pittsburgh, PA, 1987.

[96]R. J. Fordham, R. A. McCauley, K. M. Friederich, and U. Dworak, "Hot Gaseous Corrosion of Silicon Nitrides in Carburising, Sulphidising, and Oxidising Environments"; pp. 745–52 in *Ceramic Materials and Components for Engines*, Proceedings of the Second International Symposium. Edited by W. Bunk and H. Hausner. Verlag Deutsche Keramische Gesellschaft, Bad Honnef, Germany, 1986.

[97]F. C. Oliveira, R. A. H. Edwards, R. J. Fordham, and F. L. Riley, "High-Temperature Corrosion of Si_3N_4–Y_2O_3–Al_2O_3 Ceramics in $H_2S/H_2O/H_2$ Reducing Environments"; pp. 53–68 in *High-Temperature Corrosion of Technical Ceramics*. Edited by R. J. Fordham. Elsevier, New York, 1990.

[98]J. E. Marra, E. R. Kriedler, N. S. Jacobson, and D. S. Fox, "Reactions of Silicon-Based Ceramics in Mixed Oxidation Chlorination Environments," *J. Am. Ceram. Soc.*, **71** [12] 1067–73 (1988).

[99]S. Y. Ip, M. J. McNallan, and D. S. Park, "Active Oxidation of SiC-Based Ceramics in Ar–2% Cl_2–O_2 Gas Mixtures at 1000°C," *J. Am. Ceram. Soc.*, **75** [7] 1942–48 (1992).

[100]Z. Zheng, R. E. Tressler, and K. E. Spear, "The Effects of Cl_2 on the Oxidation of Single-Crystal Silicon Carbide," *Corros. Sci.*, **33** [4] 557–67 (1992).

[101]V. Pareek and D. A. Shores, "Oxidation of Silicon Carbide in Environments Containing Potassium Salt Vapor," *J. Am. Ceram. Soc.*, **74** [3] 556–63 (1991).

[102]Z. Zheng, R. E. Tressler, and K. E. Spear, "The Effect of Sodium Contamination on Oxidation of Single-Crystal Silicon Carbide," *Corros. Sci.*, **33** [4] 545–56 (1992).

[103]Z. Zheng, R. E. Tressler, and K. E. Spear, "A Comparison of the Oxidation of Sodium-Implanted CVD Si_3N_4 with the Oxidation of Sodium-Implanted SiC-Crystals," *Corros. Sci.*, **33** [4] 569–80 (1992).

[104]W. A. Sanders and J. R. Johnston, "High-Velocity Burner Oxidation and Thermal Fatigue Behavior of Si_3N_4- and SiC-Base Ceramics to 1370°C," NASA Rept. No. TM-79040, NASA Lewis Research Center, Cleveland, OH, 1978.

[105]J. D. Cawley and R. F. Handschuh, "Phenomenological Study of the Behavior of Some Silica Formers in a High-Velocity Jet Fuel Burner," NASA Rept. No. TM-87127, NASA Lewis Research Center, Cleveland, OH, 1985.

[106]E. A. Gulbransen and S. A. Jansson, "The High-Temperature Oxidation, Reduction, and Volatilization Reactions of Silicon and Silicon Carbide," *Oxid. Met.*, **4** [3] 181–201 (1972).

[107]F. J. Kohl, D. M. Leisz, G. C. Fryburg, and C. A. Stearns, "Thermochemical Analyses of the Oxidative Vaporization of Metals and Oxides by Oxygen Molecules and Atoms," NASA Rept. No. TM X-73682, NASA Lewis Research Center, Cleveland, OH, 1977.

[108]A. H. Heuer and V. L. K. Lou, "Volatility Diagrams for Silica, Silicon Nitride, and Silicon Carbide and Their Application to High-Temperature Decomposition and Oxidation," *J. Am. Ceram. Soc.*, **73** [10] 2789–803 (1990).

[109]R. W. Bartlett, "Platinum Oxidation Kinetics with Convective Diffusion and Surface Reaction," *J. Electrochem. Soc.*, **114** [6] 547–50 (1967).

[110]N. S. Jacobson, "High-Temperature Durability Considerations for the HSCT Combustor," NASA Rept. No. TP-3162, NASA Lewis Research Center, Cleveland, OH, 1991.

[111]G. H. Geiger and R. H. Poirier, *Transport Phenomena in Metallurgy*; p. 244. Addison-Wesley, Reading, MA, 1974.

[112]W. B. Hillig, "Prospects for Ultra-High-Temperature Ceramic Composites"; p. 699 in *Tailoring Multiphase and Composite Ceramics*. Edited by R. E. Tressler, G. L. Messing, C. G. Pantano, and R. E. Newnham. Plenum, New York, 1986.

[113]T. M. Besmann, "SOLGASMIX-PV: A Computer Program to Calculate Equilibrium Relationships in Complex Chemical Systems," Rept. No. ORNL/TM-5775, Oak Ridge National Laboratory, Oak Ridge, TN, 1977.

[114]C. S. Tedmon, Jr., "The Effect of Oxide Volatilization on the Oxidation Kinetics of Cr and Fe–Cr Alloys," *J. Electrochem. Soc.*, **113** [8] 766–68 (1966).

[115]E. T. Turkdogan, P. Grieveson, and L. S. Darken, "Enhancement of Diffusion-Limited Rates of Vaporization of Metals," *J. Phys. Chem.*, **67**, 1647–54 (1963).

[116]J. W. Hinze and H. C. Graham, "The Active Oxidation of Si and SiC in the Viscous Gas-Flow Regime," *J. Electrochem. Soc.*, **123** [7] 1066–73 (1976).

[117]C. Wagner, "Passivity during the Oxidation of Silicon at Elevated Temperatures," *J. Appl. Phys.*, **29** [9] 1295–98 (1958).

[118]S. C. Singhal, "Thermodynamic Analysis of the High-Temperature Stability of Silicon Nitride and Silicon Carbide," *Ceram. Int.*, **2** [3] 123–30 (1976).
[119]T. Narushima, T. Goto, and T. Hirai, "Active-to-Passive Transition in the Oxidation of CVD-SiC"; pp. 295–300 in *Composites; Corrosion/Coatings of Advanced Materials*. Edited by S. Kimura and M. Doyama. Materials Research Society, Pittsburgh, PA, 1989.
[120]K. Nickel, "The Role of Condensed Silicon Monoxide in the Active-to-Passive Oxidation Transition of Silicon Carbide," *J. Eur. Ceram. Soc.*, **9**, 3–8 (1992).
[121]P. Rocabois, C. Chatillon, and C. Benard, "Vapor Pressure and Evaporation Coefficient of SiO(amorphous) and $SiO_2(s)$ + Si(s) Mixtures by the Multiple Knudsen Cell Mass Spectrometric Method"; to appear in Proceedings of the 7th International High-Temperature Materials Properties Conference (IUPAC), Orleans, France, June 17–20, 1991.
[122]J. E. Antill and J. B. Warburton, "Active-to-Passive Transition in the Oxidation of SiC," *Corros. Sci.*, **11**, 337–42 (1971).
[123]W. L. Vaughn and H. G. Maahs, "Active-to-Passive Transition in the Oxidation of Silicon Carbide and Silicon Nitride in Air," *J. Am. Ceram. Soc.*, **73** [6] 1540–43 (1990).
[124]D. P. Butt, R. E. Tressler, and K. E. Spear, Corrosion of SiC Materials in N_2–H_2–CO Gaseous Environments: I, Thermodynamics and Kinetics of Reactions," *J. Am. Ceram. Soc.*, **75** [12] 3257–67 (1992).
[125]D. P. Butt, R. E. Tressler, and K. E. Spear, "Corrosion of SiC Materials in N_2–H_2–CO Gaseous Environments: II, Durability and Mechanical Properties," *J. Am. Ceram. Soc.*, **75** [12] 3268–77 (1992).
[126]G. H. Schiroky, "Oxidation Behavior of Chemically Vapor-Deposited Silicon Carbide," *Adv. Ceram. Mater.*, **2** [2] 137–41 (1987).
[127]N. S. Jacobson, K. N. Lee, and D. S. Fox, "Reactions of SiC and SiO_2 at Elevated Temperatures," *J. Am. Ceram. Soc.*, **75** [6] 1603–11 (1992).
[128]R. A. Rapp, "Chemistry and Electrochemistry of the Hot Corrosion of Metals," *Corros. Sci.*, **42** [10] 568–77 (1986).
[129]F. S. Pettit and C. S. Giggins, "Hot Corrosion"; pp. 327–54 in *Superalloys II*. Edited by C. T. Sims, N. S. Stoloff, and W. C. Hagel. Wiley, New York, 1987.
[130]N. S. Jacobson, J. L. Smialek, and D. S. Fox, "Molten Salt Corrosion of SiC and Si_3N_4"; pp. 99–136 in *Handbook of Ceramics and Composites*, Vol. 1, Synthesis and Properties. Edited by N. P. Cheremisinoff. Marcel Dekker, New York, 1990.
[131]W. C. Say, J. K. Wu, and W. L. Chen, "Hot Corrosion of α-SiC Ceramics by V_2O_5 Melt," *J. Mater. Sci.*, **25**, 1614–17 (1990).
[132]N. S. Jacobson, C. A. Stearns, and J. L. Smialek, "Burner Rig Corrosion of SiC at 1000°C," *Adv. Ceram. Mater.*, **1** [2] 154–61 (1986).
[133]D.-Z. Shi and R. A. Rapp, "The Solubility of SiO_2 in Fused Na_2SO_4 at 900°C," *J. Electrochem. Soc.*, **133** [4] 849–50 (1986).
[134]G. W. Watt, R. E. Andresen, and R. A. Rapp, "A Comparison of Reference Electrodes in Molten Sodium Sulfate"; p. 81 in *Molten Salts*. Edited by J. Braunstein and J. R. Selman. The Electrochemical Society, Pennington, NJ, 1981.
[135]M. McNallan, M. van Roode, and J. R. Price, "The Mechanism of High-Temperature Corrosion of SiC in Flue Gases from Aluminum Remelting Furnaces"; pp. 181–91 in Ceramic Transactions, Vol. 10, *Corrosion and Corrosive Degradation of Ceramics*. Edited by R. E. Tressler and M. McNallan. American Ceramic Society, Westerville, OH, 1990.
[136]M. A. Lamkin, F. L. Riley, and R. J. Fordham, "Hot Corrosion of Silicon Nitride in the Presence of Sodium and Vanadium Compounds"; pp. 181–91 in *High-Temperature Corrosion of Technical Ceramics*. Edited by R. J. Fordham. Elsevier Applied Science, London, U.K., 1990.
[137]S. Brooks and D. B. Meadowcroft, "The Corrosion of Silicon-Based Ceramics in a Residual Oil Fired Environment," *Proc. Br. Ceram. Soc.*, **26**, 237–50 (1978).
[138]T. Sato, S. Terauchi, T. Endo, and M. Shimada, "Corrosion of Si_3N_4 and Sialons in V_2O_5 Melts," *J. Mater. Sci.*, **25**, 1231–36 (1990).
[139]M. K. Ferber and V. J. Tennery, "Evaluation of Tubular Ceramic Heat Exchanger Materials in Acidic Coal Ash for Coal-Oil-Mixture Combustion," Rept. No. ORNL/TM-7958, Oak Ridge National Laboratory, Oak Ridge, TN, 1981.
[140]M. I. Mayer and F. L. Riley, "Sodium-Assisted Oxidation of Reaction-Bonded Silicon Nitride," *J. Mater. Sci.*, **13**, 1319–28 (1978).
[141]A. G. Evans, "Perspective on the Development of High-Toughness Ceramics," *J. Am. Ceram. Soc.*, **73** [2] 187–206 (1990).
[142]R. T. Bhatt, "Oxidation Effects on the Mechanical Properties of SiC-Fiber-Reinforced Reaction-Bonded Silicon Nitride Matrix Composites," NASA Rept. No. TM-102360, NASA Lewis Research Center, Cleveland, OH, 1989.
[143]L. Filipuzzi, G. Camus, R. Naslain, and J. Thebault, "Oxidation Mechanisms and Kinetics of 1D-SiC/C/SiC Composite Materials: I, An Experimental Approach," *J. Am. Ceram. Soc.*, in review.
[144]L. Filipuzzi and R. Naslain, "Oxidation Mechanisms and Kinetics of 1D-SiC/C/SiC Composite Materials: II, Modeling," *J. Am. Ceram. Soc.*, in review.
[145]T. E. Easler, R. C. Bradt, and R. E. Tressler, "Strength Distributions of SiC Ceramics After Oxidation and Oxidation Under Load," *J. Am. Ceram. Soc.*, **64** [12] 731–34 (1981).
[146]K. Jakus, J. E. Ritter, Jr., and W. P. Rogers, "Strength of Hot-Pressed Silicon Nitride After High-Temperature Exposure," *J. Am. Ceram. Soc.*, **67** [7] 472–75 (1984).
[147]P. F. Becher, "Strength Retention in SiC Ceramics After Long-Term Oxidation," *J. Am. Ceram. Soc.*, **66** [8] C-120–C-121 (1983).
[148]J. L. Smialek and N. S. Jacobson, "Mechanism of Strength Degradation for Hot Corrosion of α-SiC," *J. Am. Ceram. Soc.*, **69** [10] 741–52 (1986).
[149]G. A. Gogotsi, Yu. G. Gogotsi, V. P. Zavada, and V. V. Traskovsky, "Stress Corrosion of Silicon Nitride Based Ceramics," *Ceram. Int.*, **15**, 305–10 (1989).
[150]J. J. Swab and G. L. Leatherman, "Strength of Structural Ceramics after Exposure to Sodium Sulfate," *J. Eur. Ceram. Soc.*, **5**, 333–40 (1989).
[151]W. J. Tomlinson and D. M. Caslin, "Strength of SiC and SiC–7.5 vol% TiB_2 Composite after Corrosion with Na_2SO_4 and NaCl Deposits," *Ceram. Int.*, **17**, 61–66 (1991).
[152]R. E. Tressler, "Environmental Effects on Long-Term Reliability of SiC and Si_3N_4 Ceramics"; pp. 99–123 in Ceramic Transactions, Vol. 10, *Corrosion and Corrosive Degradation of Ceramics*. Edited by R. E. Tressler and M. McNallan. American Ceramic Society, Westerville, OH, 1990.
[153]K. G. Nickel, R. Danzer, G. Schneider, and G. Petzow, "Corrosion and Oxidation of Advanced Ceramics," *Powder Metall. Int.*, **21** [3] 29–34 (1989).
[154]C. H. Henager, Jr., and R. H. Jones, "Molten Salt Corrosion of Hot-Pressed Si_3N_4/SiC-Reinforced Composites and Effects of Molten Salt Exposure on Slow Crack Growth of Hot-Pressed Si_3N_4"; pp. 197–210 in Ceramic Transactions, Vol. 10, *Corrosion and Corrosive Degradation of Ceramics*. Edited by R. E. Tressler and M. McNallan. American Ceramic Society, Westerville, OH, 1990.
[155]S. M. Wiederhorn, "Moisture-Assisted Crack Growth in Ceramics," *Int. J. Fract. Mech.*, **4** [2] 171–77 (1968).
[156]L. Filipuzzi, G. Camus, J. Thebault, and R. Naslain, "Effect of High-Temperature Ageing Treatments on the Mechanical Behaviour of Unidirectional SiC/SiC Fibrous Composites"; in Proceedings of the 11th Riso International Symposium on Metallurgy and Materials Science: Structural Ceramics—Processing, Microstructure, and Properties. Edited by J. J. Bentzen *et al.* Riso National Laboratory, Roskilde, Denmark, 1990.

Nathan S. Jacobson is a senior research scientist in the Materials Division at the NASA Lewis Research Center. He received his B.A. degree in chemistry from the University of California at San Diego in 1975. He received his M.S. and Ph.D. degrees in materials science from the University of California at Berkeley in 1978 and 1981, respectively. From 1981 to 1983, Dr. Jacobson was a post-doctoral fellow at the University of Pennsylvania. Since 1983, he has been with the Environmental Durability Group of the NASA Lewis Research Center, doing research on the oxidation and corrosion of ceramics and metals at high temperatures. His current research is focused on high-temperature interfacial reactions and vaporization processes, as limiting factors in applications of ceramics and composites. In 1992, he received a NASA Exceptional Scientific Achievement Medal for his contributions to the corrosion of ceramics. Dr. Jacobson has authored or coauthored more than 50 technical papers.